ARTICLE IN PRESS

Biochemical and Biophysical Research Communications xxx (2009) xxx–xxx

Contents lists available at ScienceDirect

Biochemical and Biophysical Research Communications

journal homepage: www.elsevier.com/locate/ybbrc

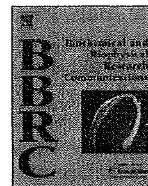

Dopamine facilitates α-synuclein oligomerization in human neuroblastoma SH-SY5Y cells

Kentaro Yamakawa [a], Yasuhiko Izumi [b], Hiroki Takeuchi [c], Noriyuki Yamamoto [b], Toshiaki Kume [b], Akinori Akaike [b], Ryosuke Takahashi [c], Shun Shimohama [c,d], Hideyuki Sawada [a,*]

[a] Clinical Research Center, Utano National Hospital, National Hospital Organization, Kyoto 616-8255, Japan
[b] Department of Pharmacology, Graduate School of Pharmaceutical Sciences, Kyoto University, Kyoto, Japan
[c] Department of Neurology, Graduate School of Medicine, Kyoto University, Kyoto, Japan
[d] Department of Neurology, School of Medicine, Sapporo Medical University, Hokkaido, Japan

ARTICLE INFO

Article history:
Received 29 October 2009
Available online xxxx

Keywords:
α-Synuclein
Oligomer
Aggregation
Dopamine
Size exclusion chromatography
Parkinson's disease

ABSTRACT

Parkinson's disease is characterized by selective loss of dopaminergic neurons in the substantia nigra and by the appearance of Lewy bodies. Fibrillar α-synuclein is the main component of Lewy bodies. Previous studies have suggested that dopamine promotes α-synuclein oligomerization and that partially aggregated or oligomeric α-synuclein could be cytotoxic. To confirm this hypothesis using cell cultures, we performed size exclusion chromatography as a pretreatment method prior to Western blotting to more clearly detect a small amount of α-synuclein oligomers in wild-type α-synuclein-overexpressing SH-SY5Y cells. Using this method, we confirmed that stable overexpression of α-synuclein in SH-SY5Y cells indeed increased the amounts of α-synuclein oligomers in these cells and exposure of the cells to dopamine for 6 h facilitated α-synuclein oligomerization. These dopamine-induced α-synuclein oligomers continued to exist for the following 24 h. However, the dopamine-treated cells did not undergo cell death or apoptosis in spite of the presence of increased oligomeric α-synuclein. Our data may contribute to the understanding of the mechanisms underlying α-synuclein oligomer formation and its suspected cytotoxicity toward dopaminergic neurons.

© 2009 Elsevier Inc. All rights reserved.

Introduction

Parkinson's disease (PD) is among the most prevalent neurodegenerative disorders. It is characterized by selective loss of dopaminergic neurons in the mesencephalic substantia nigra and by the presence of cytoplasmic inclusions, namely Lewy bodies.

One of the key molecules involved in the pathogenesis of PD is α-synuclein, the major component of Lewy bodies. α-Synuclein is a 140-amino acid protein, which exists predominantly in presynaptic nerve terminals in the brain [1,2]. Physiologically, it adopts a soluble, unfolded structure [3]; however, in the pathological state, it is supposed to aggregate and form fibrillar deposits within Lewy bodies [4].

Mutations [E46K, A53T], duplication or triplication of the α-synuclein gene increase the propensity of α-synuclein to aggregate and are linked to autosomal-dominant-inherited PD [4]. These findings again imply that aggregation and accumulation of α-synuclein are critical in the pathogenesis of PD. α-Synuclein polymerizes from soluble monomers, to dimers, trimers or oligomers, eventually becoming fibrillar aggregates. It has been hypothesized that, among these aggregated α-synuclein species, α-synuclein oligomers might be toxic to cells [5].

Previous studies have shown that dopamine promotes aggregation of monomeric α-synuclein and stabilizes oligomeric species of α-synuclein both in cell-free systems [6,7] and cultured cells [8,9]. However, in cultured cells, it is technically difficult to detect α-synuclein oligomers only by Western blotting (WB), especially when these are of wild-type α-synuclein. The purpose of this study was to determine whether dopamine promotes wild-type α-synuclein aggregation and whether aggregated α-synuclein has cytotoxicity in cultured cells. Because wild-type α-synuclein exists mainly as a soluble monomer in cells, and the amount of α-synuclein oligomers is thought to be far less than the amount of monomer, we separated cell lysates by size exclusion chromatography (SEC) prior to WB to differentiate α-synuclein oligomers from monomers. Using this method, we studied the interactions between dopamine and α-synuclein aggregation and cytotoxicity in human dopaminergic neuroblastoma SH-SY5Y cells.

Materials and methods

Materials. α-Synuclein, GBR 12935, anti-α-tubulin antibody and protease inhibitor cocktail (P8340) were purchased from Sigma

* Corresponding author. Fax: +81 75 464 0027.
E-mail address: sawada@unh.hosp.go.jp (H. Sawada).

0006-291X/$ - see front matter © 2009 Elsevier Inc. All rights reserved.
doi:10.1016/j.bbrc.2009.11.015

ARTICLE IN PRESS

(St. Louis, MO). Dopamine hydrochloride was purchased from Nacalai Tesque (Kyoto, Japan). Gel filtration standards were purchased from Bio-Rad (Hercules, CA). Rabbit polyclonal anti-α-synuclein antibody was purchased from Santa Cruz Biotechnology (sc-7011R, Santa Cruz, CA). Anti-cleaved caspase-3 antibody (Cell Signaling Technology, Beverly, MA) was used to detect caspase-3 activation. The lactate dehydrogenase (LDH) release assay was carried out using the Cytotoxicity Detection LDH kit from Kyokuto Pharmaceutical Industrial (Tokyo, Japan).

Plasmid construction. Plasmid construction was performed as previously reported [10]. α-Synuclein cDNA was amplified from postmortem human brain samples by RT-PCR using *Kpn*I- and *Xba*I-tailed primers complementary to the human α-synuclein coding region (GenBank AY049786). The nucleotide sequences of sense and antisense primers were as follows: 5′-CGGGGTACCTG GCCATTCGACGACAGTGT-3′ (sense), 5′-TGCTCTAGAGGATGGAACAT CTGTCAGCA-3′ (antisense). Appropriate restriction digestion of the PCR-amplified product was performed and the wild-type sequence was then cloned into the pcDNA3.1(+) vector (Invitrogen, San Diego, CA). Plasmid DNA was subsequently transformed into DH5α cells (Toyobo, Osaka, Japan). The resulting colonies were screened by PCR, and positives were selected, grown in liquid medium, and sequenced to verify the wild-type α-synuclein sequence (data not shown).

Stable transfection. The human dopaminergic neuroblastoma cell line SH-SY5Y was maintained at 37 °C in a humidified atmosphere of 5% CO_2 in Dulbecco's modified Eagle's medium supplemented with 10% fetal bovine serum, 2 mM glutamine, 100 U/mL penicillin, and 100 μg/mL streptomycin. When cells reached 80% confluency in 60-mm culture dishes, the medium was changed to Opti-MEM I (Invitrogen) and cells were transfected with 8 μg of wild-type α-synuclein DNA constructs using 10 μg of Lipofectamine 2000 (Invitrogen). After incubating the cells for 24 h, positive clones were selected using G418 (1300 μg/mL) for 2 weeks. Single cells were cloned in 96-well tissue culture plates. Stable transfectants established from these clones were evaluated for α-synuclein expression using Western blot analysis and immunocytochemistry.

Cell culture. SH-SY5Y cells were maintained in Opti-MEM I supplemented with 10% fetal bovine serum and incubated at 37 °C in a humidified atmosphere of 95% air and 5% CO_2. Cells were seeded in 24-well culture plates for the LDH release assay, or in 100-mm dishes for WB or SEC. Cells were grown for 72 h and then exposed to drugs.

LDH release assay for determination of viability of SH-SY5Y cells. The viability of SH-SY5Y cells was determined by LDH release assay, as described previously [11]. The activity of LDH released into the medium during the exposure to drugs was measured using a LDH assay kit. Aliquots (25 μL) of culture supernatants were mixed with 75 μL of the LDH substrate mixture contained in the assay kit. After incubation for 1 h at room temperature, the reaction was stopped by adding 100 μL of 1 N hydrochloride (HCl) and the absorbance was measured at 570 nm. LDH release from the cultured cells was evaluated as a percentage of the total LDH released following exposure to 1 mM hydrogen peroxide for 24 h.

HPLC-ED analysis of dopamine. Dopamine concentrations were measured by high-performance liquid chromatography with electrochemical detection (HPLC-ED). SH-SY5Y cells were washed twice with cold phosphate-buffered saline (PBS) and scraped in 1 mL of PBS. Cells were then centrifuged at 5000 rpm for 5 min, and homogenized in 300 μL of solubilizing buffer (0.1 N perchloric acid, 10 mM sodium disulfite, 1 mM ethylene diamine tetraacetic acid–disodium salt (EDTA–2Na) by sonication. After centrifugation at 15,000*g* for 15 min at 4 °C, the supernatants were collected for HPLC. Aliquots (10 μL) of the supernatants were analyzed by HPLC-ED. The HPLC system (HTEC-500, Eicom, Kyoto, Japan) consisted of a pump, a degasser, a column oven and an electrochemical detector with a graphite working electrode. The working electrode was maintained at an oxidative potential of +450 mV vs. an Ag/AgCl reference electrode to detect dopamine. The separation of dopamine from other endogenous compounds was achieved on a reversed-phase column (Eicompak CA-5ODS, Eicom) using a mixture of 0.1 M phosphate buffer (pH 6.0) and methanol (88:12, v/v) containing 600 mg/L sodium 1-octanesulfonate and 50 mg/L EDTA–2Na as a mobile phase. The column temperature was kept at 25 °C and the mobile phase was delivered at a flow rate of 0.23 mL/min.

Size exclusion chromatography and subsequent Western blotting. SH-SY5Y cells were washed twice with cold PBS and scraped in 1 mL of PBS. Cells were then centrifuged at 5000 rpm for 5 min, and homogenized in PBS by sonication. After centrifugation at 15,000*g* for 30 min at 4 °C, supernatants were filtered through a 0.2 μm hydrophilic PTFE disposable membrane (Millex-LG, Millipore). Protein concentrations were determined using Bradford's assay (Bio-Rad) and some amounts (2000–3000 μg) was loaded onto Shodex SEC columns (Showa Denko, Tokyo, Japan). The columns were equilibrated with mobile phase buffer (0.01 M Tris–HCl, pH 7.0, 0.15 M NaCl and 0.2% N-lauroylsarcosine) before analysis. Samples were eluted at a flow rate of 0.25 mL/min, and fractions were collected 1 mL per tube. The absorbance value at OD 280 nm of each fraction was used to draw the elution profile. For WB, equal volumes (10 μL) of each fraction were mixed with 2× sample buffer (0.125 M Tris–HCl, 20% glycerol, 4% sodium dodecyl sulfate (SDS), bromophenol blue), without boiling, loaded onto a 5–20% polyacrylamide gradient gel (e-PAGEL, ATTO, Tokyo, Japan) for SDS–polyacrylamide gel electrophoresis (SDS–PAGE) and transferred to polyvinylidene difluoride (PVDF) membranes (Immobilon-P^{SQ}, Millipore). The membranes were then incubated in 5% dry milk in Tris-buffered saline with Tween 20 (TBS-T, 20 mM Tris, 137 mM NaCl, 0.1% Tween 20, pH 7.6) at room temperature for 1 h and incubated with α-synuclein antibodies (1:1000 dilution) in blocking solution (3% bovine serum albumin, 0.05% sodium azide in PBS) overnight at 4 °C. The membranes were then washed four times, 10 min each, in TBS-T, followed by 1 h incubation in horse radish peroxidase (HRP) conjugated secondary antibody (1:2000 dilution). The membranes were next washed six times, 10 min each, in TBS-T before incubation in chemiluminescence reagents (ECl plus, GE Healthcare) and then exposed to film. All procedures were performed on ice.

The SEC system consisted of a system controller (SCL-10A_{VP}, Shimadzu, Kyoto, Japan), a degasser (DGU-14A, Shimadzu), a solvent delivery (LC-10AT_{VP}, Shimadzu), an auto-sampler (SIL-10AD_{VP}, Shimadzu), a column oven (CTO-10AC_{VP}, Shimadzu), a guard column (KW-G; Showa Denko), Shodex silica-based columns (KW-802.5, KW-803, Showa Denko), a photodiode array detector (SPD-M10A_{VP}, Shimadzu), a fraction collector (FRC-10A, Shimadzu) and a sample cooler. For better separation, three silica-based columns were lineated (from the upper side, KW-803, KW-803, and KW-802.5 in this sequence). Data acquisition and processing were carried out using Class VP software (Shimadzu). The SEC conditions were as follows: injection volume 500 μL (including 2000–3000 μg of protein), flow rate 0.25 mL/min, column temperature 25 °C, sample cooler temperature 4 °C.

Western blotting for cleaved caspase-3. SH-SY5Y cells were harvested as described above and homogenized in lysis buffer (0.02 M Tris, pH 7.0, 25 mM β-glycerophosphate, 2 mM EGTA, 1% Triton X-100, with a 1% protease inhibitor cocktail) by sonication. After centrifugation at 15,000*g* for 30 min at 4 °C, supernatants were collected and protein concentrations were determined. Twenty micrograms of each sample was mixed with 2× sample buffer (0.125 M Tris–HCl, 20% glycerol, 4% SDS, 31 mg/mL dithiothreitol, bromophenol blue), boiled for 5 min, loaded on a 5–20% polyacrylamide gradient gel for SDS–PAGE and transferred to PVDF

Please cite this article in press as: K. Yamakawa et al., Dopamine facilitates α-synuclein oligomerization in human neuroblastoma SH-SY5Y cells, Biochem. Biophys. Res. Commun. (2009), doi:10.1016/j.bbrc.2009.11.015

membranes. The membranes were incubated with anti-cleaved caspase-3 antibody (1:1000 dilution) and appropriate HRP-conjugated secondary antibodies (1:2000 dilution). Immunoreactive proteins on membranes were visualized with ECl plus.

Statistical analysis. The statistical significance of the differences among three or more groups of individual data was analyzed by one-way analysis of variance (ANOVA) and a post hoc multiple comparison using Dunnett's test. Statistical significance was defined as $P < 0.05$. Data are expressed as means ± SEM.

Results

Detection of α-synuclein oligomers by size exclusion chromatography and subsequent Western blotting

The silica-based columns used here gave linear elution profiles of a set of protein standards having molecular weights of 1.35–670 kDa, indicating efficient column separation (Fig. 1A). The elution profiles of wild-type α-synuclein-overexpressing SH-SY5Y cells for monomeric and oligomeric α-synuclein are shown in Fig. 1B. α-Synuclein monomer, dimer, trimer, and tetramer bands were detected mainly in fractions 27, 25, 24, and 23, respectively (Fig. 1B). Monomeric bands were also detected in these oligomers fractions, suggesting that SDS dissolved the oligomeric α-synuclein to monomer. A higher molecular weight smear was also detected (Fig. 1B). By contrast, the elution profiles of untransfected cells showed smaller amounts of endogenous α-synuclein monomer with only slightly detectable oligomer bands (Fig. 1C).

Dopamine facilitated α-synuclein oligomerization and its effect is suppressed by a DAT inhibitor

Next we examined the effect of dopamine on α-synuclein oligomerization in wild-type α-synuclein-overexpressing SH-SY5Y cells. To this end, we first investigated the cellular content of dopamine when cells were exposed to dopamine. Wild-type α-synuclein-overexpressing cells were exposed to 100 μM dopamine for 45 min in the presence or absence of 3.2 μM GBR 12935, a dopamine transporter (DAT) inhibitor. Dopamine concentrations in cell lysates were measured by HPLC. While no detectable amount of dopamine was found in untreated cells, it was detected in dopamine-treated cells (Fig. 2A). In addition, co-administration of 3.2 μM GBR 12935 with dopamine significantly reduced the cellular content of dopamine, indicating that extracellular dopamine was taken up by cells via the dopamine transporter. We examined the elution profiles of dopamine-treated cells for α-synuclein. Wild-type α-synuclein-overexpressing cells were incubated in the presence or absence of 100 μM dopamine for 6 h and cell lysates were separated by SEC. To compare the subtle difference in the amount of α-synuclein oligomer, equal volumes (10 μL) of fractions 19–25 of sham- and dopamine-treated samples were analyzed by SDS–PAGE in a single 5–20% gradient gel, and immunoblotted for α-synuclein. When the elution profiles of dopamine-treated cell lysates (Fig. 2B, right half of the gel) were compared with that of sham treatment (Fig. 2B, left half of the gel), the intensities of oligomeric α-synuclein bands in fractions 21–23 were apparently increased (Fig. 2B and C). Furthermore, the intensities of monomeric α-synuclein bands in fraction 21–23 were also slightly increased (Fig. 2B, right half of the gel), indicating that a portion of dopamine-induced oligomers was denatured by SDS (Fig. 2B and C). These changes, however, could not be detected when the same samples were immunoblotted without SEC, suggesting that SEC worked as an efficient pretreatment method before WB to detect small amounts of dopamine-induced α-synuclein oligomers (Fig. 2D). When the cells were co-treated with dopamine and GBR 12935, the increase in the amount of α-synuclein oligomers was suppressed (Fig. 2E). Overall, these findings suggested that dopamine was taken up by the dopamine trans-

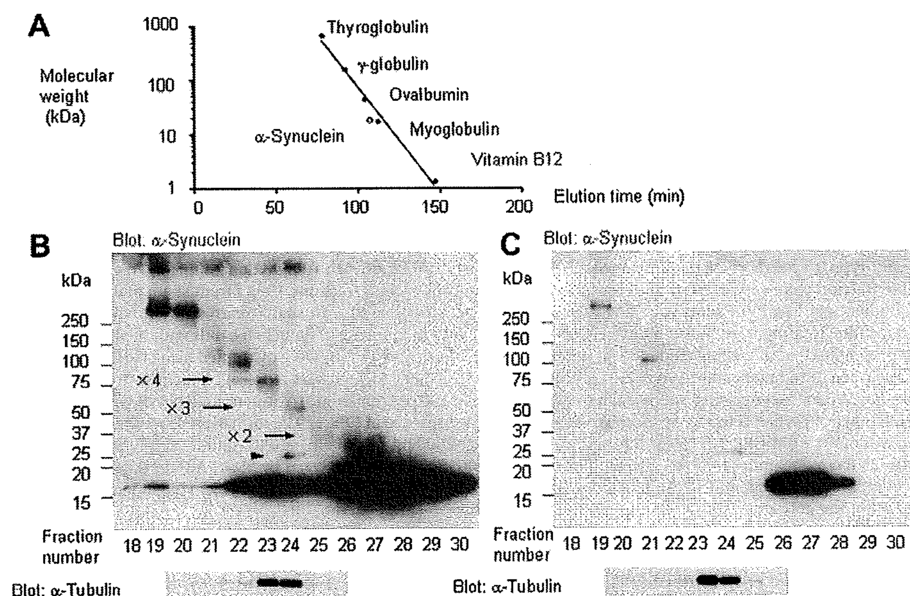

Fig. 1. Elution profiles of SEC (A) and detection of α-synuclein oligomers in SH-SY5Y cells (B, C). (A) Calibration curve for SEC. The linearity of the calibration curve indicates efficient column separation. Protein size markers and molecular weights are as follows: thyroglobulin (670 kDa), γ-globulin (158 kDa), ovalbumin (44 kDa), myoglobin (17 kDa), and vitamin B12 (1.35 kDa) (filled circles). Recombinant monomeric α-synuclein (18 kDa) is shown as an open circle. (B, C) Detection of α-synuclein oligomeric bands in SH-SY5Y cells. Equal amounts (2000 μg of protein) of the PBS-soluble cell lysates were separated by SEC and 10 μL of each collected fraction was analyzed by SDS–PAGE in 5–20% gradient gels. The PVDF blots were analyzed for α-synuclein (upper panel) and re-blotted for α-tubulin as a loading control (lower panel). (B) Cell lysates from wild-type α-synuclein-overexpressing SH-SY5Y cells were analyzed. Films were exposed for long enough to detect trace oligomeric bands, so the monomeric α-synuclein bands were saturated. α-Synuclein dimer, trimer, and tetramer were detected (arrow). The 25-kDa band in fraction 24 (arrowhead) was a non-specific band. Higher molecular species were also detected. (C) Cell lysates from untransfected SH-SY5Y cells were analyzed. The film exposure time was the same as in (B). Note, endogenous α-synuclein monomer was detected in fraction 27.

Please cite this article in press as: K. Yamakawa et al., Dopamine facilitates α-synuclein oligomerization in human neuroblastoma SH-SY5Y cells, Biochem. Biophys. Res. Commun. (2009), doi:10.1016/j.bbrc.2009.11.015

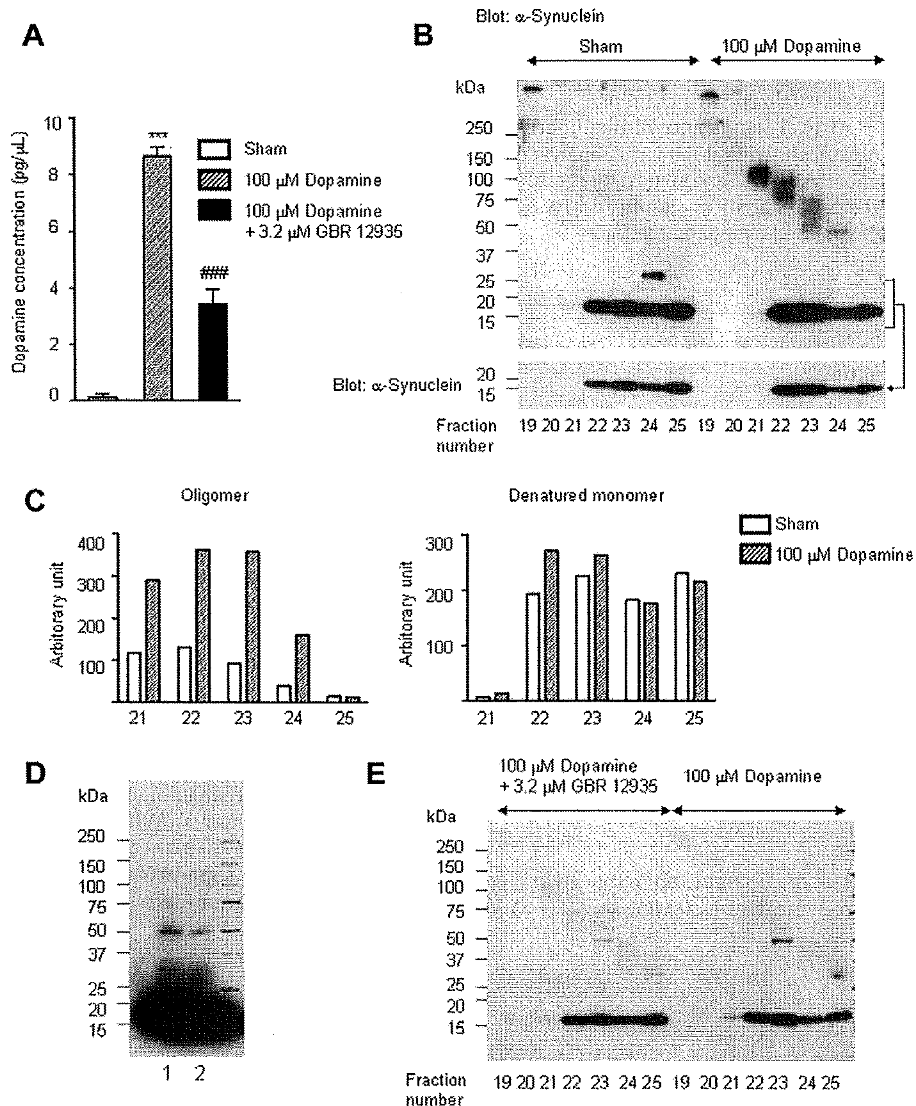

Fig. 2. Dopamine content (A) and α-synuclein oligomerization (B–E) after dopamine treatment. (A) Intracellular uptake of dopamine via the dopamine transporter. Wild-type α-synuclein-overexpressing SH-SY5Y cells were exposed to 100 μM dopamine for 45 min in the presence or absence of GBR 12935. Cells were collected in PBS and homogenized in 300 μL of solubilizing buffer. After centrifugation at 15,000g for 15 min at 4 °C, supernatants were analyzed for dopamine content by HPLC. $^{***}P < 0.001$ compared with sham treatment. $^{\#\#\#}P < 0.001$ compared with dopamine alone. $n = 3$ dish/experiment. Data were expressed as means ± SEM. (B) Dopamine facilitated α-synuclein oligomerization in wild-type α-synuclein-overexpressing SH-SY5Y cells. Cells were exposed to 100 μM dopamine for 6 h and equal amounts (3000 μg of protein) of cell lysate from the PBS-soluble fraction were separated by SEC. Ten-microliter aliquots of each of fractions 19–25 from sham and dopamine treatments were analyzed by SDS–PAGE in a single 5–20% gradient gel. The PVDF blots were analyzed for α-synuclein. Compared with sham treatment (left half of the gel), the amounts of α-synuclein oligomers were increased by dopamine treatment (right half of the gel). Lower panel shows monomeric α-synuclein bands with the film exposed for a shorter time than in the upper panel. The results are representative of three independent experiments. (C) The blots shown in (B) were quantified using NIH ImageJ software for the relative amounts of α-synuclein oligomers and their denatured monomers. White bars represent sham treatment. Striped bars represent dopamine treatment. (D) The same samples as shown in (B), before SEC, were analyzed by WB for α-synuclein. Lane 1, sham treatment. Lane 2, 100 μM dopamine treatment for 6 h. WB without SEC could not detect any difference in the amount of α-synuclein oligomer. (E) When cells were exposed to dopamine in the presence of GBR 12935, formation of α-synuclein was suppressed. Cells were exposed to 100 μM dopamine with or without 3.2 μM GBR 12935 for 6 h, and same amount (2000 μg of protein) of PBS-soluble cell lysate was separated by SEC. Ten-microliter aliquots of each of fractions 19–25 from dopamine-treated cells, with or without GBR 12935, were analyzed by SDS–PAGE in the same 5–20% gradient gel. The PVDF blots were stained for α-synuclein. Compared with dopamine treatment alone (right half of the gel), the amounts of α-synuclein oligomers were decreased by dopamine treatment with 3.2 μM GBR 12935 (left half of the gel).

porter and facilitated wild-type α-synuclein oligomerization in cells.

α-Synuclein oligomer continued to exist in cells up to 24 h after washing out dopamine-containing medium but did not cause cell death

Because it has been hypothesized that α-synuclein oligomers are cytotoxic, we investigated the effect of dopamine-induced α-synuclein oligomers on cell viability. To this end, wild-type α-synuclein-overexpressing SH-SY5Y cells were exposed to 100 μM dopamine for 6 h and incubated in dopamine-free medium for a further 24 h. The elution profile of dopamine washout treatment showed that almost the same amount of α-synuclein oligomer was still found in the cells after 24 h of washout time, compared with no washout treatment (Fig. 3A). An LDH release assay revealed that cells were viable after 24 h washout time (Fig. 3B). In addition, though staurosporine-induced apoptotic cells

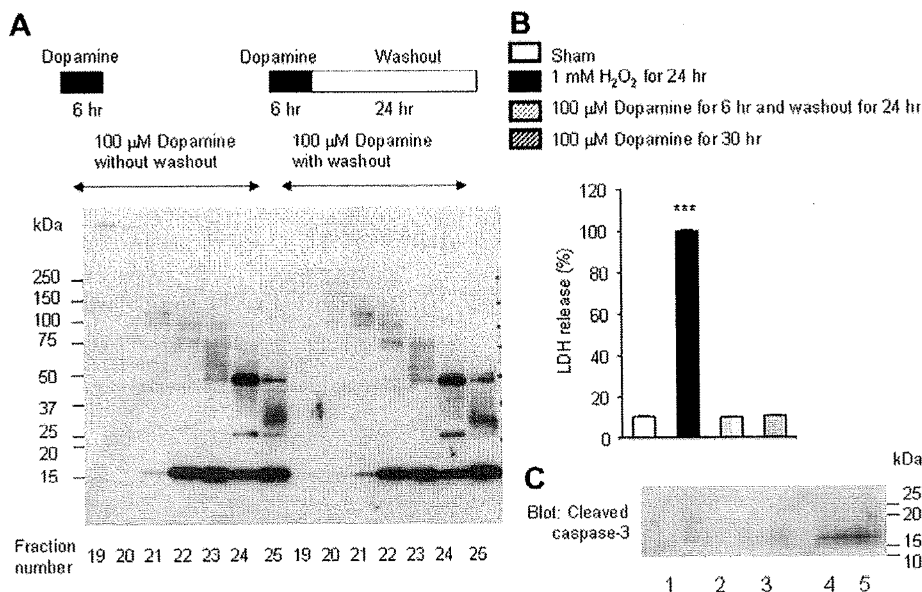

Fig. 3. Twenty-four hours-persistent oligomers in cells and their cytotoxicity (A–C). (A) Dopamine-induced α-synuclein oligomers existed in cells after removal of dopamine from the medium for 24 h. α-Synuclein-overexpressing SH-SY5Y cells were exposed to 100 μM dopamine for 6 h. After that, cells were incubated in dopamine-free medium for a further 24 h. The same amount (2000 μg of protein) of cell lysate was separated by SEC and 10 μL aliquots of each of fractions 19–25 from dopamine-treated cells with or without 24 h washout treatment were analyzed for α-synuclein. Almost the same amount of α-synuclein oligomer still existed after removal of dopamine for 24 h (right half of the gel), compared with dopamine treatment for 6 h (left half of the gel). (B) An LDH assay showed that the dopamine-treated cells with oligomeric α-synuclein did not undergo cell death within the following 24 h. Wild-type α-synuclein-overexpressing SH-SY5Y cells were exposed to 100 μM dopamine for 6 h. After that, the cells were incubated in dopamine-free medium for further 24 h. No difference in LDH release was found between sham treatment and dopamine treatment. $^{***}P < 0.001$ compared with sham treatment. $n = 4$ dish/experiment. Data were expressed as means ± SEM. (C) Caspase-3 was not activated in dopamine-treated cells with oligomeric α-synuclein. α-Synuclein-overexpressing SH-SY5Y cells were treated with dopamine or staurosporine and analyzed by WB for cleaved caspase-3. Cleaved caspase-3 levels did not increase following dopamine treatment. Lane 1, control. Lane 2, treatment with 100 μM dopamine for 6 h. Lane 3, treatment with 100 μM dopamine for 6 h with 24 h washout time. Lane 4, treatment with 0.25 μM staurosporine for 3 h. Lane 5, treatment with 0.25 μM staurosporine for 6 h.

caused cleavage of caspase-3, this was not observed in dopamine-treated cells (Fig. 3C). These findings suggested that neither cell death nor apoptosis had occurred, in spite of the fact that α-synuclein oligomers still existed in the cells.

Discussion

In this study, we adopted the combined methods of SEC and WB to detect wild-type α-synuclein oligomers in cells. Although we could not distinguish α-synuclein oligomers from α-synuclein bound to other proteins, their molecular weights and sequential separation by SEC suggested that these bands with oligomeric molecular weights included α-synuclein oligomers. Previous studies have analyzed cell lysates of α-synuclein-overexpressing cells by combining SEC and WB [8,12]; however, only monomeric wild-type α-synuclein bands, but not oligomeric bands, were detected in these studies. In our study, oligomeric α-synuclein bands themselves, especially tetramers were detected. It is said that in most cell models the recovered α-synuclein is predominantly monomeric on SDS–PAGE gels [13]. We suspect that this might reflect, in part, the nature of α-synuclein oligomers that are sensitive to SDS or heating. Therefore, in this study, the non-boiling sample preparation condition may have helped make the detection of α-synuclein oligomer bands easier. Another means of detecting oligomeric α-synuclein is delipidation treatment. Sharon et al. [14] reported that α-synuclein oligomers could also be detected by simple WB with non-boiled samples (from mouse brains) when heat was added to blotted PVDF membranes or samples were delipidated, and therefore, that some α-synuclein oligomers were not detected by WB because they were bound to lipid in cells. Therefore, lipid-bound α-synuclein was not detected in this study.

Exposure of α-synuclein-overexpressing cells to dopamine promoted oligomerization of α-synuclein. These data were consistent with the findings of previous studies using recombinant α-synuclein [6,7] or cultured cells [8,9]. They reveal that dopamine promotes the formation of SDS-resistant α-synuclein oligomers within 5 min [7] to 3 days [6] in a cell-free system or within 3–5 days [8,9] in cells. We demonstrated that intracellular oligomerization was facilitated by dopamine within 6 h, and that the oligomers were stable for at least 24 h.

A previous study using A53T mutant- and tyrosine hydroxylase mutant-overexpressing SH-SY5Y cells revealed that α-synuclein oligomers were innocuous [8]. These results are consistent with our study. However, it has been controversial whether over-expressed α-synuclein, some part of which may be oligomerized as shown in Fig. 2, is cytotoxic or innocuous [13]. Therefore, the cytotoxicity of oligomeric α-synuclein requires confirmation in further experiments.

In conclusion, we demonstrated that dopamine promotes wild-type α-synuclein oligomerization in cells and that these α-synuclein oligomers did not cause cytotoxicity, at least up to 24 h. Further study is needed to elucidate the relationship between α-synuclein oligomerization and Parkinson's disease.

References

[1] R. Jakes, M.G. Spillantini, M. Goedert, Identification of two distinct synucleins from human brain, FEBS Lett. 345 (1994) 27–32.
[2] A. Iwai, E. Masliah, M. Yoshimoto, N. Ge, L. Flanagan, H.A. de Silva, A. Kittel, T. Saitoh, The precursor protein of non-A beta component of Alzheimer's disease amyloid is a presynaptic protein of the central nervous system, Neuron 14 (1995) 467–475.
[3] P.H. Weinreb, W. Zhen, A.W. Poon, K.A. Conway, P.T. Lansbury Jr., NACP, a protein implicated in Alzheimer's disease and learning, is natively unfolded, Biochemistry 35 (1996) 13709–13715.

ARTICLE IN PRESS

[4] E.A. Waxman, B.I. Giasson, Molecular mechanisms of alpha-synuclein neurodegeneration, Biochim. Biophys. Acta 1792 (2009) 616–624.
[5] M.J. Volles, P.T. Lansbury Jr., Zeroing in on the pathogenic form of alpha-synuclein and its mechanism of neurotoxicity in Parkinson's disease, Biochemistry 42 (2003) 7871–7878.
[6] K.A. Conway, J.C. Rochet, R.M. Bieganski, P.T. Lansbury Jr., Kinetic stabilization of the alpha-synuclein protofibril by a dopamine-alpha-synuclein adduct, Science 294 (2001) 1346–1349.
[7] R. Cappai, S.L. Leck, D.J. Tew, N.A. Williamson, D.P. Smith, D. Galatis, R.A. Sharples, C.C. Curtain, F.E. Ali, R.A. Cherny, J.G. Culvenor, S.P. Bottomley, C.L. Masters, K.J. Barnham, A.F. Hill, Dopamine promotes alpha-synuclein aggregation into SDS-resistant soluble oligomers via a distinct folding pathway, FASEB J. 19 (2005) 1377–1379.
[8] J.R. Mazzulli, A.J. Mishizen, B.I. Giasson, D.R. Lynch, S.A. Thomas, A. Nakashima, T. Nagatsu, A. Ota, H. Ischiropoulos, Cytosolic catechols inhibit alpha-synuclein aggregation and facilitate the formation of intracellular soluble oligomeric intermediates, J. Neurosci. 26 (2006) 10068–10078.
[9] C.E. Moussa, F. Mahmoodian, Y. Tomita, A. Sidhu, Dopamine differentially induces aggregation of A53T mutant and wild type alpha-synuclein: insights into the protein chemistry of Parkinson's disease, Biochem. Biophys. Res. Commun. 365 (2008) 833–839.
[10] R. Kohno, H. Sawada, Y. Kawamoto, K. Uemura, H. Shibasaki, S. Shimohama, BDNF is induced by wild-type alpha-synuclein but not by the two mutants, A30P or A53T, in glioma cell line, Biochem. Biophys. Res. Commun. 318 (2004) 113–118.
[11] Y. Izumi, H. Sawada, N. Sakka, N. Yamamoto, T. Kume, H. Katsuki, S. Shimohama, A. Akaike, *p*-Quinone mediates 6-hydroxydopamine-induced dopaminergic neuronal death and ferrous iron accelerates the conversion of *p*-quinone into melanin extracellularly, J. Neurosci. Res. 79 (2005) 849–860.
[12] J. Xu, S.Y. Kao, F.J. Lee, W. Song, L.W. Jin, B.A. Yankner, Dopamine-dependent neurotoxicity of alpha-synuclein: a mechanism for selective neurodegeneration in Parkinson disease, Nat. Med. 8 (2002) 600–606.
[13] M.R. Cookson, M. van der Brug, Cell systems and the toxic mechanism(s) of alpha-synuclein, Exp. Neurol. 209 (2008) 5–11.
[14] R. Sharon, I. Bar-Joseph, M.P. Frosch, D.M. Walsh, J.A. Hamilton, D.J. Selkoe, The formation of highly soluble oligomers of alpha-synuclein is regulated by fatty acids and enhanced in Parkinson's disease, Neuron 37 (2003) 583–595.

Please cite this article in press as: K. Yamakawa et al., Dopamine facilitates α-synuclein oligomerization in human neuroblastoma SH-SY5Y cells, Biochem. Biophys. Res. Commun. (2009), doi:10.1016/j.bbrc.2009.11.015

Neuroscience Research xxx (2009) xxx–xxx

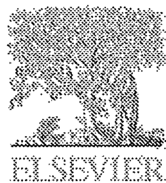

Contents lists available at ScienceDirect

Neuroscience Research

journal homepage: www.elsevier.com/locate/neures

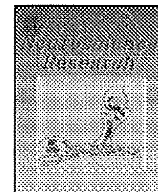

Loss of PINK1 in medaka fish (*Oryzias latipes*) causes late-onset decrease in spontaneous movement

Hideaki Matsui[a,b], Yoshihito Taniguchi[b,c], Haruhisa Inoue[a,b], Yoshito Kobayashi[a], Yoshiyuki Sakaki[d,1], Atsushi Toyoda[d,2], Kengo Uemura[a,b], Daisuke Kobayashi[e], Shunichi Takeda[b,c,*], Ryosuke Takahashi[a,b,**]

[a] *Department of Neurology, Kyoto University, Graduate School of Medicine, 54 Shogoin-Kawahara-cho, Sakyo-ku, Kyoto 606-8507, Japan*
[b] *Core Research for Evolutional Science and Technology (CREST), Japan Science and Technology Agency, Japan*
[c] *Department of Radiation Genetics, Kyoto University, Graduate School of Medicine, Yoshida-Konoe-cho, Sakyo-ku, Kyoto 606-8501, Japan*
[d] *RIKEN Genomic Sciences Center, Yokohama 230-0045, Japan*
[e] *Department of Anatomy and Developmental Biology, Kyoto Prefectural University of Medicine, Kyoto 602-0841, Japan*

ARTICLE INFO

Article history:
Received 21 May 2009
Received in revised form 16 October 2009
Accepted 23 October 2009
Available online xxx

Keywords:
Parkinson's disease
PTEN-induced kinase 1 (*PINK1*)
Medaka fish (*Oryzias latipes*)
TILLING (targeted induced local lesions in genomes)
Dopamine
Movement disorder

ABSTRACT

Parkinson's disease is a neurodegenerative disease associated with the degeneration of dopaminergic neurons in the substantia nigra. The PTEN-induced kinase 1 gene (*PINK1*) is responsible for recessive inherited familial Parkinson's disease (PARK6). Neither the function of PINK1 nor its role in the prevention of Parkinson's disease is fully understood. Gene disruption of *PINK1* causes remarkably different phenotypes in animal models such as *Drosophila melanogaster*, zebrafish, and mouse, none of which recapitulate Parkinson's-disease-like symptoms. We established *PINK1*-gene-disrupted medaka fish. These mutant fish grew normally at first, then developed significant decrease in the frequency of spontaneous swimming movements in the late-adult stage. Although the mutants did not show any dopaminergic cell loss, the amount of 3,4-dihydroxyphenylacetic acid, a major metabolite of dopamine, decreased. Thus, PINK1 contributes to the maintenance of dopamine metabolism, even before the selective death of dopaminergic neurons. Our animal model is therefore a valuable tool to detect pathogenesis in Parkinson's patients in the early stages.

© 2009 Elsevier Ireland Ltd and the Japan Neuroscience Society. All rights reserved.

1. Introduction

Parkinson's disease (PD) is the second-most common neurodegenerative disease among humans. It is associated with the degeneration of dopaminergic neurons in a subset of neuronal populations represented by the substantia nigra pars compacta in the midbrain. Although the majority of cases develop sporadically, 5–10% of PD patients are familial, with the disease caused by gene mutation (Gasser, 2005). To date, 10 different genes responsible for familial PD have been identified. The functional analysis of these genes is important to our understanding of the molecular pathogenesis of PD. Recessive inherited familial PD (PARK6) is attributable to mutations in the *PINK1* gene (Valente et al., 2004). These mutations appear to compromise the function of the PINK1 protein (Sim et al., 2006).

PINK1 is a highly conserved 581 amino acid protein. The gene is ubiquitously expressed in the human brain (Gandhi et al., 2006) and seems to be activated by a tumor suppressor, PTEN (Unoki and Nakamura, 2001). The *PINK1* gene encodes a kinase and contains a mitochondria-targeting motif. One of the putative substrates of the kinase is TNF receptor-associated protein 1 (TRAP1), though its biological significance remains elusive (Pridgeon et al., 2007). PINK1 plays a protective role against oxidative stress and MPTP (Wood-Kaczmar et al., 2008; Haque et al., 2008). Silencing of the *PINK1* gene results in mitochondrial pathology in the human cell line (Exner et al., 2007).

Gene disruption of *PINK1* causes distinctly different phenotypes in different animal models. Mice deficient in PINK1 exhibit impaired dopamine release, but not movement disorders or dopaminergic cell death (Kitada et al., 2007). Loss of PINK1 function in *Drosophila melanogaster* results in a drastic phenotype that includes male sterility and the degeneration of both muscle and dopaminergic neurons with massive mitochondria-related pathology (Clark et al., 2006; Park et al., 2006; Yang et al., 2006). In

* Corresponding author at: Department of Radiation Genetics, Kyoto University, Graduate School of Medicine, Yoshida-Konoe-cho, Sakyo-ku, Kyoto 606-8501, Japan.
** Corresponding author at: Department of Neurology, Kyoto University, Graduate School of Medicine, 54 Shogoin-Kawahara-cho, Sakyo-ku, Kyoto 606-8507, Japan.
E-mail addresses: stakeda@rg.med.kyoto-u.ac.jp (S. Takeda), ryosuket@kuhp.kyoto-u.ac.jp (R. Takahashi).
[1] Present address: Toyohashi University of Technology, 1-1, Hibarigaoka, Tenpaku-cho, Toyohashi, Aichi 441-8580, Japan.
[2] Present address: Comparative Genomics Laboratory, National Institute of Genetics, Yata 1111, Mishima, Shizuoka 411-8540, Japan.

0168-0102/$ – see front matter © 2009 Elsevier Ireland Ltd and the Japan Neuroscience Society. All rights reserved.
doi:10.1016/j.neures.2009.10.010

Please cite this article in press as: Matsui, H., et al., Loss of PINK1 in medaka fish (*Oryzias latipes*) causes late-onset decrease in spontaneous movement. Neurosci. Res. (2009), doi:10.1016/j.neures.2009.10.010

zebrafish, depletion of PINK1 during development causes severe developmental disorders and neurodegeneration (Anichtchik et al., 2008). None of these animal models for PARK6 faithfully recapitulate the pathology of human PD.

In this study, we generated *PINK1* mutant medaka fish by screening our TILLING library (Taniguchi et al., 2006). The *PINK1* mutant medaka showed normal phenotypes for germ-cell lineage, skeletal muscle, and mitochondrial morphology. However, they showed a significant decrease in spontaneous movement during the late stages of life as well as deregulation of dopamine metabolism. The *PINK1* mutant medaka therefore provides a unique opportunity to analyze the causal relationship between dopamine metabolism and neurological symptoms.

2. Materials and methods

2.1. Cloning of medaka PINK1 gene

RNA was extracted from *wild-type* medaka embryos by Trizol (Invitrogen) according to the manufacturer's instructions. cDNA was synthesized using SuperScript III (Invitrogen). To identify medaka *PINK1* orthologs, we used the basic local alignment search tool (BLAST) to search the medaka genome database (http://dolphin.lab.nig.ac.jp/medaka/). Medaka *PINK1* cDNA sequences were then determined using a combination of RT-PCR and rapid amplification of cDNA ends (RACE). RACE products were generated using Seegene's Capfishing kit (Seegene). The 5′ RACE (CCATAGGC-CAAGGGCTTGAGCGGGC) and 3′ RACE primers (CCAGTGCCCCC-GCTGATGTGCAGTTAGT) were used. The cDNA sequence was used to retrieve the genomic sequence from the draft medaka genome assembly.

2.2. Generation of PINK1 mutant medaka

Generation of *PINK1* mutant medaka was carried out as described previously (Taniguchi et al., 2006). To find the mutations in the region of interest, the genome sequence was amplified with forward primer #1 (TCGGCTTCTACAAGGCTGTT) and reverse primer #1 (CACCCAACTGTGGCTAGTGA) by PCR (92 °C for 60 s; 12 cycles of 92 °C for 20 s, 65 °C for 20 s with a decrement of 0.6 °C per cycle, 72 °C for 30 s; 20 cycles of 92 °C for 20 s, 58 °C for 20 s and 72 °C for 30 s; 72 °C for 180 s [T1 Thermocycler, Biometra]). Sequences were analyzed for the presence of heterozygous mutations using the reverse primer #1. *In vitro* fertilization was carried out using sperm with the desired mutation and the progeny were genotyped by sequencing. Heterozygous fish carrying the same mutation were back-crossed with *Kyoto-Cab*, a substrain of *Cab*, at least 4 times. Furthermore, all the experiments were reproduced using fish back-crossed 7 times or more. Heterozygous fish with this mutation were incrossed to obtain homozygous fish. To verify the genotype of the progeny from this incross, the genome was amplified with forward primer #2 (CAGATTGG-GAAAGGATCCAA) and reverse primer #2 (CCCAAAGTTCCACAG-CATCT). PCR was carried out according to the following thermocycling program: 94 °C for 120 s; 35 cycles of 94 °C for 30 s, 62 °C for 30 s, 72 °C for 30 s; and 72 °C for 120 s (GeneAmp PCR system9700, Applied Biosystems). 1 μl of PCR product was used as a template for sequencing using BigDYE (Applied Biosystems). Sequencing products were purified by magnetic beads and analyzed using the ABI 3700 DNA Sequencer (Applied Biosystems), following the standard protocol.

2.3. Semi-quantitative RT-PCR

RNA was extracted from the brain for each genotype with Trizol (Invitrogen). cDNA was synthesized using 1 μg RNA for each genotype with SuperScript III (Invitrogen). mRNA expression levels were determined by PCR. For *PINK1*, PCR was carried out using the following thermocycling program: 94 °C for 120 s; 28 cycles at 94 °C for 30 s, 68 °C for 30 s, 72 °C for 30 s; and 72 °C for 120 s (T1 Thermocycler, Biometra). For *β-actin*, the thermocycling program was 94 °C for 120 s; 20 cycles at 94 °C for 30 s, 61 °C for 30 s, 72 °C for 30 s; and 72 °C for 120 s (T1 Thermocycler, Biometra). Forward primer #3 (GAACAGAGCCGTCTTTCTGG) and reverse primer #3 (CCCAAAGTTCCACAGCATCT) were used for *PINK1*. The forward primer (ACTACCTCATGAAGATCCTG) and the reverse primer (TTGCTGATCCACATCTGCTG) were used for *β-actin*.

2.4. In situ hybridization

The digoxigenin (DIG) labeled riboprobe was generated with the DIG RNA labeling kit according to the manufacturer's instructions (Roche). Medaka brains were fixed in freshly prepared 4% paraformaldehyde in PBST. Brains were dehydrated sequentially in methanol. After rehydration, the specimens were treated with 10 μg/ml proteinase K, and treated again in the same fixative for 25 min. The specimens were pre-hybridized in hybridization buffer (HB, 50% formamide, 5× SSC, 5 mg/ml yeast tRNA, 100 μg/ml heparin, 0.1% Tween-20) at 65 °C for 2 h, and then brains were hybridized overnight with the riboprobe in hybridization buffer at 65 °C. Subsequently, brains were washed in decreasing concentrations of SSCT. For probe detection, the embryos were incubated in 0.2% blocking solution (Roche) for 2 h and then rocked overnight with anti-DIG antibody conjugated with alkaline phosphatase (1:7000 dilution, Roche) in 0.2% blocking solution at 4 °C. After several washes with PBST, hybridized probe was detected via color reaction with 450 μg/ml NBT and 175 μg/ml BCIP (Roche). The color reaction was stopped by PBST. Samples were fixed in 4% paraformaldehyde in PBST for 20 min, then embedded in paraffin. Specimens were sliced into 7 μm sections.

2.5. High performance liquid chromatography

Medaka brains were homogenized in 100 μl of 0.4 M $HClO_4$ containing 4 mM $Na_2S_2O_5$ and 4 mM diethylenetriaminepentaacetic acid. Supernatant by centrifugation at 18,500 × *g* for 5 min was used to measure free catechols. High performance liquid chromatography (HPLC) was conducted with a mobile phase containing buffer A:acetonitrile:methanol (1000:25.9:62.9, v/v) (buffer A: 0.1 M phosphate, 0.05 M citrate, 4 mM sodium 1-heptanesulfonate and 0.1 mM EDTA, pH 3.0). Catecholamine and its metabolites were identified using a series coulometric detector (ESA, Inc.). Data were collected and processed using CHROMELEON™ Chromatography Data Systems 6.40 (Dionex). The pellet was reserved for analysis of the protein content. For this purpose, the pellet was solubilized in 100 μl of 0.5N NaOH at 60 °C and the protein was quantified by means of a BCA assay (Pierce) using bovine serum albumin (BSA) as the standard.

2.6. Hematoxylin–eosin staining

Entire medaka bodies or individual organs were fixed in 4% paraformaldehyde for 24 h, embedded in paraffin, then sliced into 10-μm sections. Hematoxylin–eosin (HE) staining was done using standard protocols.

2.7. Transmission electron microscope and Toluidine blue staining

To prepare for electron microscopy, male testes and muscle tissue were fixed overnight in 2% gluteraldehyde with a 0.1 M cacodylate buffer. After rinsing in a 0.1 M cacodylate buffer with 0.1 M sucrose, samples were postfixed in 1% OsO_4, with a 0.1 M

cacodylate buffer and 0.1 M sucrose for 1.5 h. Samples were rinsed, dehydrated in an ethanol series, and embedded in Epon. The 1-μm sections were stained with Toluidine blue, and the 50–80 nm sections were stained with uranyl acetate and lead citrate.

2.8. Immunohistochemistry

Medaka brains were fixed in 4% paraformaldehyde for 24 h and embedded in paraffin. Each brain was sliced into 20 μm sections to prepare for TH immunohistochemistry. Immunohistochemical analysis (1:500, mouse anti-TH, MAB318, Millipore) was carried out on every section using the Vector Elite ABC kit with DAB. The number of dopaminergic neurons in the middle diencephalon was determined by counting the TH-immunopositive (TH^+) neurons in the coronal sections using an OLYMPUS BX51 microscope with a MICROFIRE digital camera (Olympus) and Stereo Investigator (MBF Bioscience).

2.9. TdT-mediated dUTP nick-end labeling assay

Brains were fixed in 4% paraformaldehyde for 24 h and embedded in paraffin. Each brain was sliced into 5 μm sections in preparation for a TUNEL assay. Apoptotic cells were detected by the TUNEL method using an *in situ* Apoptosis Detection Kit (TaKaRa Bio Inc.), according to the manufacturer's protocol.

2.10. Western blot analysis

Brains were homogenated in a RIPA buffer (25 mM Tris–HCl [pH 7.6], 150 mM NaCl, 1% NP-40, 1% sodium deoxycholate, 0.1% SDS) with protease inhibitors and processed for SDS-PAGE analysis. Immunoreactive bands were detected with ECL reagent or ECL plus reagent (GE Healthcare Life Sciences) and the chemiluminescent signal was visualized by exposing the membrane to Fuji RX X-ray film (Fuji Film). The film was scanned and densitometric analysis of blots was performed using ImageJ software (National Institute of Health). The background intensity of the film was subtracted from the band intensity. Anti-medaka parkin polyclonal antibody was raised against full-length medaka parkin protein and used for the analysis (1:500). Anti-TH monoclonal antibody (1:1000, mouse anti-TH, MAB318, Millipore) was used for the Western blot analysis of the TH. Anti-β-actin monoclonal antibody (1:5000, AC-15, Sigma–Aldrich) was used for the loading control. Parkin-deficient medaka, used for a negative control, was generated as described previously (Taniguchi et al., 2006).

2.11. Behavioral analysis

The medaka were tested for spontaneous swimming. Images were collected using a video camera positioned above the tank under low intensity, indirect white light, then analyzed by a computer-assisted system (Muromachi Kikai). The water tank was a transparent circular container (20 cm diameter, 2 cm water depth, 27 °C). Upon introduction into the tank, all adult fish remained motionless for several minutes, then began to swim. Filming began 1 min after the medaka began to swim and lasted for 5 min. We defined *movement* as occurring when a medaka moved more than 0.1 cm per 0.1 s. Total swimming distance (cm), duration of swimming movement (s) and swimming velocity (total swimming distance/duration of swimming movement) were measured and compared across groups.

2.12. Statistical analysis

Data were expressed as mean ± standard error of the mean (SEM). Results were statistically evaluated for significance using the ANOVA test with post hoc analysis using Dunnet's test or logrank test for survival analysis. Differences were considered significant when $p < 0.05$.

3. Results

3.1. Cloning of medaka PINK1

Only a single ortholog of the human *PINK1* gene was identified (by BLAST search) in the draft medaka genome. The medaka *PINK1* gene has 8 exons and encodes a protein consisting of 577 amino acids (Fig. 1A and B). The medaka PINK1 amino acid sequence has 54.1% homology to human PINK1. The kinase domain was highly conserved between the two species (Fig. 1B).

3.2. Generation of PINK1 mutant medaka

To generate *PINK1* mutant medaka, we targeted exons 2 and 3 of the *PINK1* gene for nucleotide sequencing. We sequenced the genomes of 5771 samples obtained from ENU-mutagenized medaka. We identified 14 mutations in total, 6 of which were silent mutations (Table 1). From the eight other mutations, we selected a nonsense mutation, Q178X, for further study because it resulted in the disruption of the kinase domain. It has been reported that human PARK6 patients carry similar truncation mutations (Q239X, R246X, Y258X, W437X, Q456X, R492X) in the kinase domain (Valente et al., 2004; Hedrich et al., 2006; Hatano et al., 2004; Tan et al., 2006).

From the incross of heterozygous Q178X mutant parents, we obtained the expected numbers (according to Mendelian inheritance [Fig. 3A]) of *wild-type* fish ($PINK1^{WT/WT}$), heterozygous mutants ($PINK1^{WT/Q178X}$), and homozygous mutants ($PINK1^{Q178X/Q178X}$) (Fig. 2A). Semi-quantitative RT-PCR showed a marked reduction of *PINK1* mRNA in the $PINK1^{Q178X/Q178X}$ medaka, probably due to the nonsense-mediated mRNA decay (Fig. 2B). We therefore concluded that we had succeeded in generating PINK1-deficient medaka fish.

3.3. Distribution of medaka PINK1 mRNA

To characterize medaka *PINK1* expression, we visualized medaka *PINK1* mRNA by *in situ* hybridization. The anti-sense RNA probe exhibited diffuse signals in the gray matter of $PINK1^{WT/WT}$ medaka brain (Fig. 4A–E). The telencephalon and diencephalon that contain striatum and many dopaminergic neurons respectively showed moderate anti-sense signals (Fig. 4A–C). The optic tectum disclosed relatively intense signals comparing to other regions (Fig. 4B and C). On the other hand, the signals of hindbrain and spinal cord were weak (Fig. 4D and E). We further investigated medaka *PINK1* mRNA expression in $PINK1^{Q178X/Q178X}$ medaka. In this case, we could not detect the signals of anti-sense probe (Fig. 4F–J). This finding suggested the signals of anti-sense probe was specific to medaka *PINK1* mRNA and again supported the degradation of *PINK1* mRNA in $PINK1^{Q178X/Q178X}$ medaka.

3.4. $PINK1^{Q178X/Q178X}$ medaka showed normal development and mild shortening of life span

Like human PARK6 patients, $PINK1^{Q178X/Q178X}$ medaka grew normally for 12 months without any obvious morphological abnormalities or developmental disorders. Remarkably, the $PINK1^{Q178X/Q178X}$ medaka showed a significant decrease in life span, when compared with $PINK1^{WT/WT}$ and $PINK1^{WT/Q178X}$ fish (the $PINK1^{Q178X/Q178X}$ medaka began to die at 12 months) (Fig. 3B). This diminished life expectancy was not caused by increased tumorigenesis (data not shown).

Please cite this article in press as: Matsui, H., et al., Loss of PINK1 in medaka fish (*Oryzias latipes*) causes late-onset decrease in spontaneous movement. Neurosci. Res. (2009), doi:10.1016/j.neures.2009.10.010

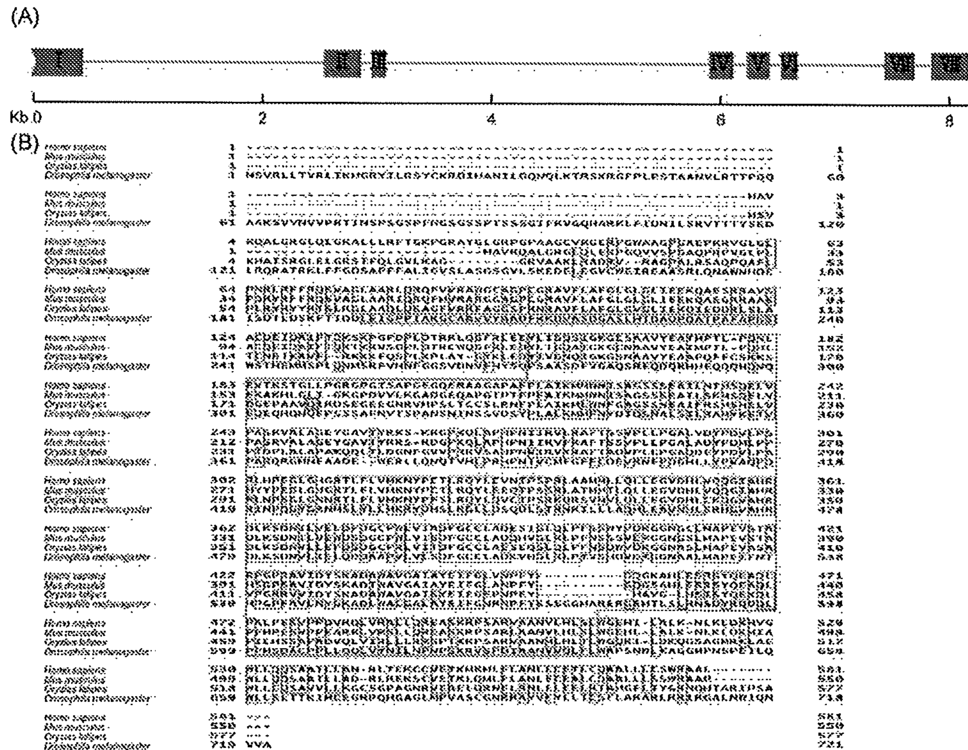

Fig. 1. Medaka PINK1 profiles. (A) Genome structure of medaka *PINK1* gene. The red boxes indicate each exon (with the Greek numeral representing the number of the exon) and the bar represents the intron. (B) Sequence alignment of human, mouse, medaka and *Drosophila melanogaster* PINK1 protein. Amino acids conserved among three or four species are outlined in red. The medaka PINK1 amino acid sequence has 54.1% homology to human PINK1. The kinase domain, which is highly conserved across the two species, is outlined in light blue. The green outlining signifies the Q178X mutation in the mutant medaka. (For interpretation of the references to color in this figure legend, the reader is referred to the web version of the article.)

3.5. *PINK1*$^{Q178X/Q178X}$ medaka show reduced body weight at the late-adult stage

To investigate the cause of this shortened life expectancy, we measured the body weight of the *PINK1*$^{Q178X/Q178X}$ medaka over time. We placed ten 8-month-old fish from each genotype into separate tanks for 4 months. There was no significant difference in body weight among medaka with the *PINK1*$^{WT/WT}$, *PINK1*$^{WT/Q178X}$, and *PINK1*$^{Q178X/Q178X}$ genotypes during this time (Fig. 5A). Nor were there significant differences in body weight when medaka representing all three genotypes were maintained together in one tank for 8 months. However, at 12 and 18 months, the body weight of the *PINK1*$^{Q178X/Q178X}$ medaka increased at a slower rate, compared with the *PINK1*$^{WT/Q178X}$ and *PINK1*$^{Q178X/Q178X}$ medaka when all the genotypes were maintained together (Fig. 5B). These findings imply that older *PINK1*$^{Q178X/Q178X}$ medaka were not able to compete for limited amounts of food with littermates carrying the other genotypes.

Table 1
List of *PINK1* mutations from our TILLING library showing mutated nucleotides and resulting changes of the transcript.

DNA sequence	Amino acid substitution	Result
AGGACACTTC (A>G) TTTACATACC		Intron
TGCAGGCGGT (G>A) TTCAGAAAGA	V121V	Silent
AAAGAAGAAG (T>C) TCCAGAGCCC	F127L	Substitution
AACTGGAGGA (T>C) TACATTGTAG	D142D	Silent
AAAGGATCCA (A>G) CGCAGCTGTG	N154S	Substitution
GCTGTGTATG (A>G) AGCTGCACCT	E159G	Substitution
CCAAGAAAAG (C>T) GATGGTGAGC	S170S	Silent
CGCCGCGGTG (C>T) AGATACGAGA	Q178X	Truncation
GCTGTGGAAC (T>C) TTGGGGTGGG	F212L	Substitution
TGTGATTCTA (T>A) GTGTTTGCAG		Intron
TTCCCACAGA (C>T) CCCCTCGCTC	D233D	Silent
CGCTCTGGCG (C>A) CAGCAAAACA	P239T	Substitution
GCTCTGGCGC (C>T) AGCAAAACAG	P239L	Substitution
CGCCAGCAAA (A>G) CAGCAACTTA	K241K	Silent

(A>B): A is the nucleotide of *wild-type* Kyoto-cab and B is the nucleotide of the mutant. Of the 14 types of mutation in the genome, 2 were located in the intron, 5 resulted in silent change of the amino acid sequence, 6 were amino acid substitutions and 1 was a truncation of the transcript. The mutation we selected (Q178X) is underlined.

3.6. Muscle, sperm, and mitochondria intact in *PINK1*$^{Q178X/Q178X}$ medaka

PINK1-deficient *Drosophila* show male sterility, skeletal muscle and sperm degeneration, and abnormal mitochondria morphology. We therefore inspected the morphology of these tissues in medaka. Contrary to the *Drosophila* model, the skeletal muscle and sperm appeared to be normal in the *PINK1*$^{Q178X/Q178X}$ medaka (Fig. 6A–D). Nor did the mitochondria in the skeletal muscle (Fig. 6E and F) or sperm show any abnormal morphology (data not shown). Both male and female *PINK1*$^{Q178X/Q178X}$ medaka were consistently fertile (data not shown). Thus, deletion of PINK1 causes a significantly less abnormal phenotype of muscle and sperm in medaka than in *Drosophila*.

3.7. Amount of parkin indistinguishable across genotypes

Familial PD (PARK2) is caused by mutations of the gene-encoding E3 ubiquitin ligase, *parkin* (Kitada et al., 1998). Since studies of the *PINK1*-silenced zebrafish and *D. melanogaster* found a reduction of *parkin* mRNA and parkin protein, respectively (Anichtchik et al., 2008; Yang et al., 2006), we used Western blot analysis to measure parkin protein. The amount of parkin was comparable in the *PINK1*$^{WT/WT}$, *PINK1*$^{WT/Q178X}$, and *PINK1*$^{Q178X/Q178X}$ medaka (Fig. 7).

Please cite this article in press as: Matsui, H., et al., Loss of PINK1 in medaka fish (*Oryzias latipes*) causes late-onset decrease in spontaneous movement. Neurosci. Res. (2009), doi:10.1016/j.neures.2009.10.010

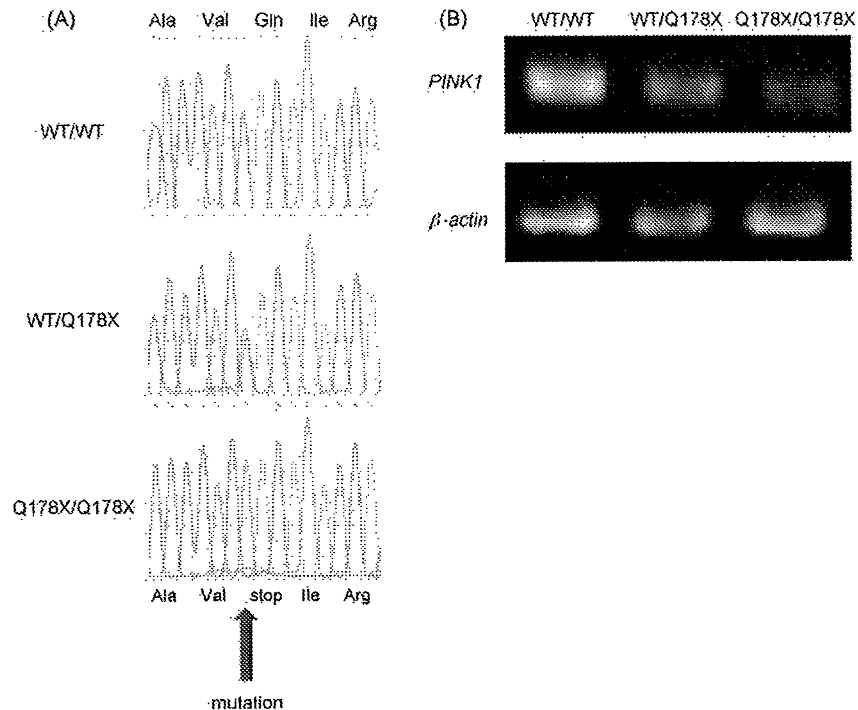

Fig. 2. Generation of $PINK1^{Q178X/Q178X}$ medakas. (A) Sequence data for each genotype. A = green, T = red, G = black, and C = blue. The three-letter amino acid codes show the resulting transcript. The top figure illustrates the $PINK1^{WT/WT}$ medaka sequence, while the middle and bottom figures illustrate heterozygous and homozygous Q178X mutation in $PINK1^{WT/Q178X}$ and $PINK1^{Q178X/Q178X}$ medaka, respectively. The C to T mutation of the genome results in a TAG stop codon (red arrow). (B) Semi-quantitative RT-PCR of *PINK1* mRNA for each genotype. The upper and lower lanes show the RT-PCR results of *PINK1* and *β-actin* (control) mRNA, respectively. The *PINK1* mRNA of the $PINK1^{Q178X/Q178X}$ medaka decreased markedly compared with $PINK1^{WT/WT}$ and $PINK1^{WT/Q178X}$. This reduction may be due to nonsense-mediated mRNA decay. (For interpretation of the references to color in this figure legend, the reader is referred to the web version of the article.)

3.8. No significant dopaminergic cell loss in $PINK1^{Q178X/Q178X}$ medaka

Dopaminergic cell loss and the denervation of the striatum constitute the representative pathology of human PD patients. Having previously identified tyrosine-hydroxylase-positive (TH^+) dopaminergic neurons and noradrenergic neurons in the medaka brain, as well as selective loss of TH^+ dopaminergic neurons in MPTP-treated medaka (Matsui et al., 2009), we histologically examined the TH^+ neurons. The number of cells in the middle diencephalon did not decrease in the $PINK1^{Q178X/Q178X}$ medaka, when compared with medaka carrying the other genotypes, even at 18 months (Fig. 8A–E). Western blot analysis of the whole brain indicated a similar amount of TH protein in each genotype (Fig. 8I). The $PINK1^{Q178X/Q178X}$ medaka did not display pathological abnormalities in dopaminergic neurons in other regions or in noradrenergic neurons in the medulla oblongata (data not shown). We continued to inspect TH immunohistochemistry, focusing on the striatum, because we previously found that the striatum contains the terminals of dopaminergic neurons, and also because denervation of the striatum is observed in human PD patients. The distribution of dopaminergic neurons in the striatum showed no detectable abnormalities in the $PINK1^{Q178X/Q178X}$ medaka (Fig. 8G and H). To analyze apoptotic cells, we performed a TUNEL assay on the whole brain. Virtually no apoptotic cell death was present in either the $PINK1^{Q178X/Q178X}$ or the control medaka (data not shown). In sum, the $PINK1^{Q178X/Q178X}$ medaka showed no prominent defect in the number or morphology of dopaminergic and noradrenergic neurons.

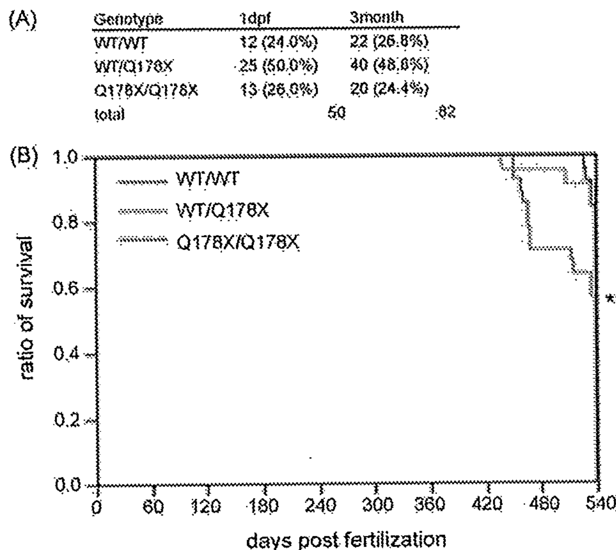
(A)

Genotype	1dpf	3month
WT/WT	12 (24.0%)	22 (26.8%)
WT/Q178X	25 (50.0%)	40 (48.8%)
Q178X/Q178X	13 (26.0%)	20 (24.4%)
total	50	82

Fig. 3. Mendelian inheritance of Q178X mutation and survival curves of $PINK1^{Q178X/Q178X}$ medaka. (A) The ratio of genotypes in newborn and 3-month-old medaka with $PINK1^{WT/Q178X}$ parents. Both results agree with Mendelian inheritance. These Mendelian ratios suggest no difference in mortality rates in the developmental/larval stage. (B) Survival curve for each genotype. End point is the death of each medaka or day 540. The results show mild but significant shortening of the life span in $PINK1^{Q178X/Q178X}$ medaka ($n = 28$), comparing with $PINK1^{WT/WT}$ ($n = 26$) or $PINK1^{WT/Q178X}$ ($n = 46$). $^{***}p < 0.001$ vs. $PINK1^{WT/WT}$.

3.9. Abnormal amount of dopamine and DOPAC in the absence of PINK1 in the brains of young and old fish

A decreased amount of catecholamine is the most prominent feature of human PD patients. We therefore measured the amount of dopamine and norepinephrine in the whole brain of $PINK1^{Q178X/Q178X}$ medaka at 4, 8, 12 and 18 months. The amount of norepinephrine did not differ across genotypes (Fig. 9C). Unlike with human PD patients, the amount of dopamine in the medaka carrying $PINK1^{Q178X/Q178X}$ as well as the other genotypes was very similar at 12 and 18 months. However, to our surprise, the amount

Please cite this article in press as: Matsui, H., et al., Loss of PINK1 in medaka fish (*Oryzias latipes*) causes late-onset decrease in spontaneous movement. Neurosci. Res. (2009), doi:10.1016/j.neures.2009.10.010

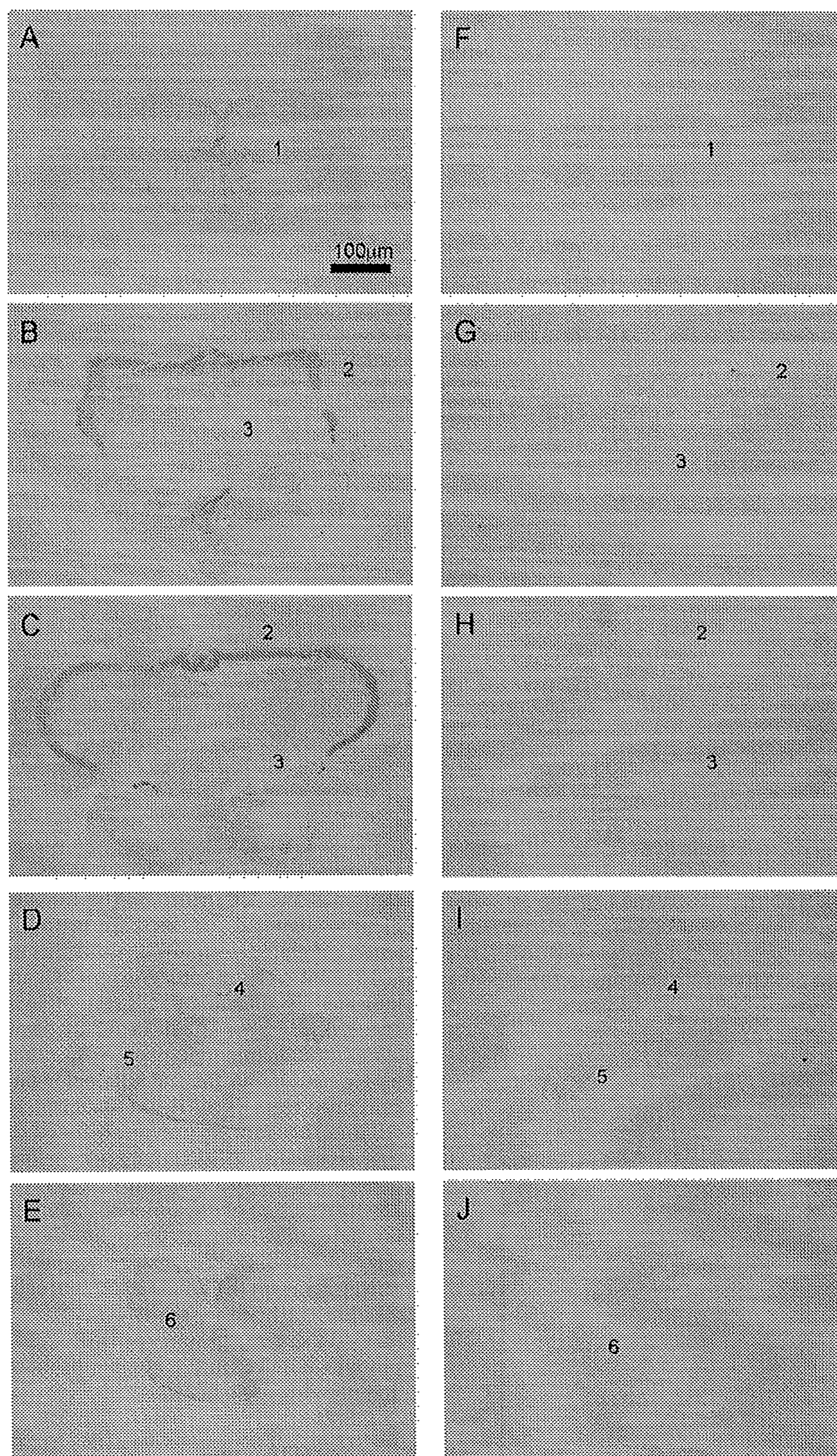

Fig. 4. *In situ* hybridization of medaka *PINK1* mRNA. Anti-sense signals of $PINK1^{WT/WT}$ medaka brain (A–E) and $PINK1^{Q178X/Q178X}$ medaka brain (F–J) (12 months). (1) Telencephalon, (2) optic tectum, (3) diencephalon, (4) cerebellum, (5) medulla oblongata and (6) spinal cord.

of dopamine in the $PINK1^{Q178X/Q178X}$ medaka brain was higher than that of the $PINK1^{WT/WT}$ at both 4 and 8 months (Fig. 9A). By 12 months, the levels of dopamine were the same for all genotypes, and they remained the same at 18 months (Fig. 9A). If the elevated dopamine were functional, these fish might be expected to move more frequently than fish carrying the other genotypes. In fact, the $PINK1^{Q178X/Q178X}$ medaka moved less frequently than did the fish carrying the other genotypes (Fig. 10A–C), suggesting that the elevated dopamine levels reflect deregulation of dopamine metabolism, including the defective release of dopamine from the neurons. This idea is supported by the fact that the amount of 3,4-dihydroxyphenylacetic acid (DOPAC), a metabolite of dopa-

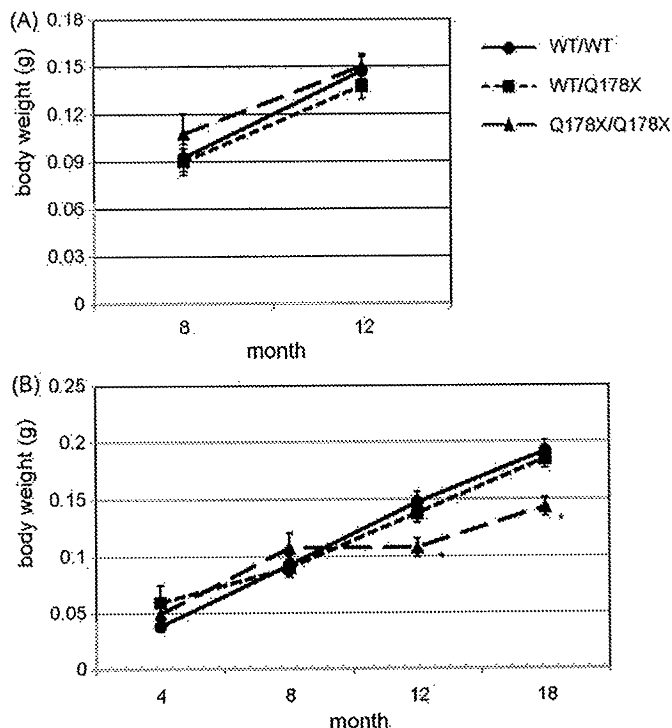

Fig. 5. Body weight of $PINK1^{Q178X/Q178X}$ medaka. (A) Body-weight curves for fish separated by genotype at 8 months. No significant differences were seen ($n = 10$ for each group). (B) Body-weight curves for fish not separated by genotype. A reduced increase in body weight was observed for the $PINK1^{Q178X/Q178X}$ medaka at 12 and 18 months ($n = 15$ for each group). $^*p < 0.05$ vs. $PINK1^{WT/WT}$.

mine, decreased. We conclude that the loss of PINK1 causes dysregulation of dopamine metabolism without affecting the survival of dopaminergic neurons.

3.10. $PINK1^{Q178X/Q178X}$ mutation causes reduction of spontaneous swimming only at 12 and 18 months

Late-onset reduction of spontaneous movement is one of the key symptoms found in human PD patients. We therefore quantified spontaneous swimming movement in $PINK1^{Q178X/Q178X}$ medaka. All fish showed comparable movement at 4 and 8 months, irrespective of the genotype of the *PINK1* gene. Remarkably, the $PINK1^{Q178X/Q178X}$ medaka displayed a significant reduction of spontaneous swimming at 12 and 18 months, in comparison with fish carrying the other genotypes (Fig. 10A–D). These significant decreases were confirmed by all examined swimming parameters: total distance, duration of movement, and velocity. We therefore conclude that the loss of PINK1 causes late-onset reduction of spontaneous swimming movement.

4. Discussion

Japanese medaka (*Oryzias latipes*) is easy to handle and produce large numbers of progeny per generation. It has several advantages over zebrafish in modeling PD. First, the whole genome has been sequenced and assembled since the size of medaka genome is only 700 Mb, half the size of the zebrafish genome. Second, several inbred strains have been established in medaka, but not in zebrafish. The lack of genetic variations among individuals may simplify and facilitate genetic studies, and is particularly important for disease models. Third, cryopreservation of the sperm is easy and reliable, so we can maintain and store numerous strains in the laboratory. Considering the merits that are above-mentioned, we can regard medaka as one of the attractive vertebrate (*Drosophila* is not vertebrate) animal models.

In this report, we verified that the $PINK1^{Q178X/Q178X}$ medaka is a novel animal model suitable for use to investigate the pathogenesis of PD. Mutant fish display a phenotype very close to that of human PD patients. This phenotype includes normal development and growth, mild shortening of the life span, late-onset reduction of spontaneous movement, and a decrease in the amount of dopamine metabolic product (DOPAC). The establishment of the medaka PD model will allow for extensive genetic analysis in the future, using multiple gene disruption and expression of transgenes with large numbers of fish.

By analyzing the medaka PD model over time, we were able to determine the level of dopamine and its metabolic products in the brain. We found that the loss of PINK1 function affects the metabolism of dopamine in the central nervous system. Indeed, the amount of DOPAC decreased between the 4 and 18 months. Unexpectedly, we observed a higher, rather than a lower, amount of dopamine in the brains of 4- and 8-month-old $PINK1^{Q178X/Q178X}$ medaka compared to $PINK1^{WT/WT}$. This appears to be similar to the results of a study using *PINK1*-shRNA-expressing transgenic mice, which showed increased amounts of dopamine (Zhou et al., 2007). In another study, gene disruption of *PINK1* was found to impair the release of dopamine from neurons in the striatum, though the dopamine levels were not documented (Kitada et al., 2007). In our study, the increased level of dopamine was not associated with an increase in spontaneous movement in young $PINK1^{Q178X/Q178X}$ medaka. Taking these observations together, it seems that one possible scenario is that the $PINK1^{Q178X/Q178X}$ medaka are incapable of effectively releasing dopamine as a neuronal transmitter, leading to the accumulation of dopamine in the neuronal cells. This accumulated dopamine might harm the neurons, because the metabolism of dopamine is accompanied by the generation of oxidative radical species (Blum et al., 2001). Whether or not the amount of dopamine also increases in the brain of human PARK6 patients prior to the appearance of PD-related symptoms should be investigated.

The late-adult-onset phenotype of the $PINK1^{Q178X/Q178X}$ medaka is in marked contrast with the more prominent phenotypes of PINK1-depleted zebrafish and *D. melanogaster*. In zebrafish, the Morpholino-mediated suppression of PINK1 caused developmental disorders as well as neurodegeneration (Anichtchik et al., 2008). This severe phenotype of PINK1-depleted zebrafish is surprising. The different phenotypes of the two models might be attributable to the difference of species or strategies. Morpholino may have off-target effect (Ekker and Larson, 2001). On the other hand, non-negligible mutations by ENU may remain although backcross progeny have been analyzed. In *D. melanogaster*, the loss of PINK1 resulted in selective defects in dopaminergic neurons, skeletal muscle, sperm, and mitochondria. It should be noted that the phenotype associated with the loss of PINK1 is distinctly different in model animals such as medaka, zebrafish, mouse, and *D. melanogaster*. The genetic study of *Drosophila* provides compelling evidence that PINK1 works in the same pathway as does parkin. In fact, the loss of function in parkin, *PINK1*, or both genes will result in the same pathology in *Drosophila* (Clark et al., 2006; Park et al., 2006; Yang et al., 2006). An important question that needs to be solved in near future is whether the genetic relationship demonstrated in *Drosophila* is also observed in other PD model animals, including medaka.

Diffuse signal pattern of medaka *PINK1* mRNA in the gray matter is consistent with that of rat and mouse *PINK1* (Taymans et al., 2006). The distribution of *PINK1* mRNA is not restricted to the dopaminergic neurons in rat, mouse and our medaka fish. This makes it difficult to explain why loss of PINK1 function leads to the dysfunctions of dopaminergic neurons. The ways to prove the

Please cite this article in press as: Matsui, H., et al., Loss of PINK1 in medaka fish (*Oryzias latipes*) causes late-onset decrease in spontaneous movement. Neurosci. Res. (2009), doi:10.1016/j.neures.2009.10.010

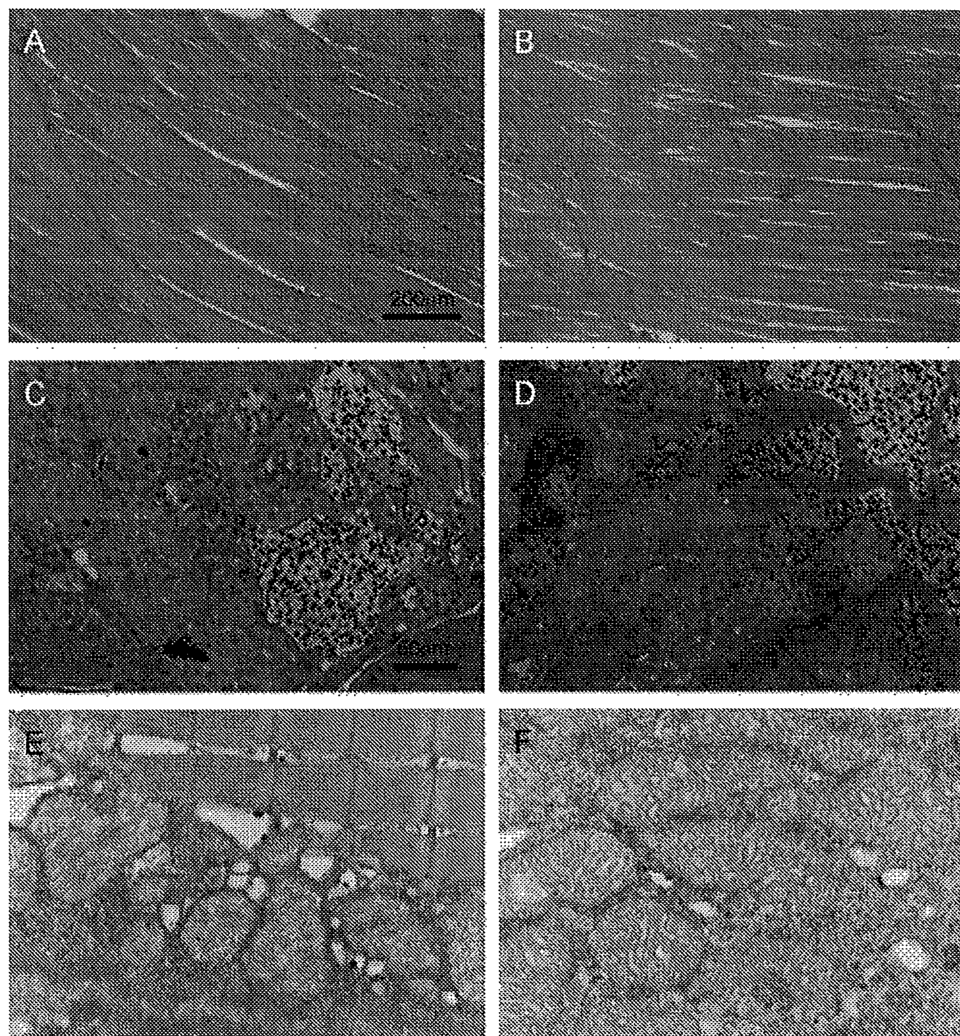

Fig. 6. Histological analysis of muscle and testes in *PINK1*$^{Q178X/Q178X}$ medaka fish (12 months). (A, C, and E) PINK1$^{WT/WT}$. (B, D, and F) *PINK1*$^{Q178X/Q178X}$. (A and B) Hematoxilin–eosin staining of the muscle. (C and D) Toluidine blue staining of the testes. (E and F) Electron-microscopic image of mitochondria in the muscle. (A–F) Muscles, testes and mitochondria are intact in the *PINK1*$^{Q178X/Q178X}$ medaka. (F) Altered cristae morphology, fragmentation or elongation of mitochondria were not detected. (For interpretation of the references to color in this figure legend, the reader is referred to the web version of the article.)

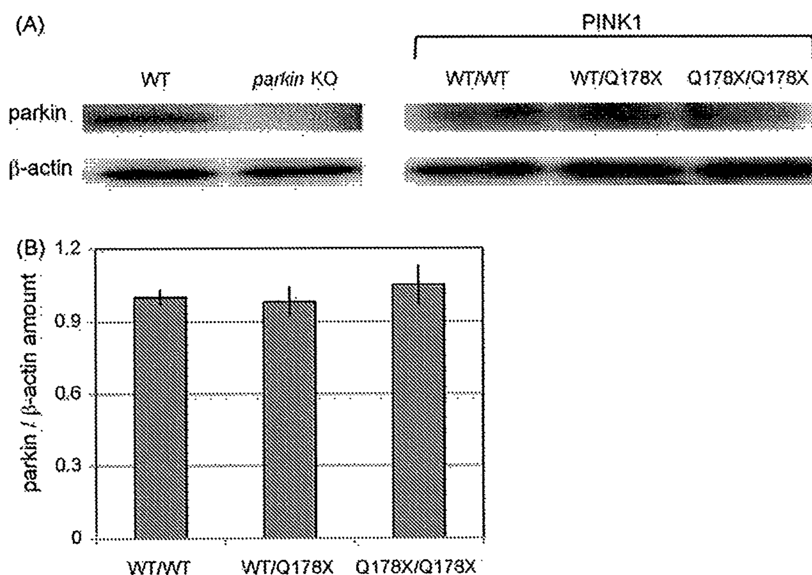

Fig. 7. Amount of parkin protein in *PINK1*$^{Q178X/Q178X}$ medaka (18 months). (A) Amount of protein in medaka parkin examined by Western blot analysis. (B) Ratio of parkin/β-actin (loading control) for each genotype (average amount for *PINK1*$^{WT/WT}$ medaka = 1). The amount of parkin does not differ across genotypes ($n = 6$ for each group).

Please cite this article in press as: Matsui, H., et al., Loss of PINK1 in medaka fish (*Oryzias latipes*) causes late-onset decrease in spontaneous movement. Neurosci. Res. (2009), doi:10.1016/j.neures.2009.10.010

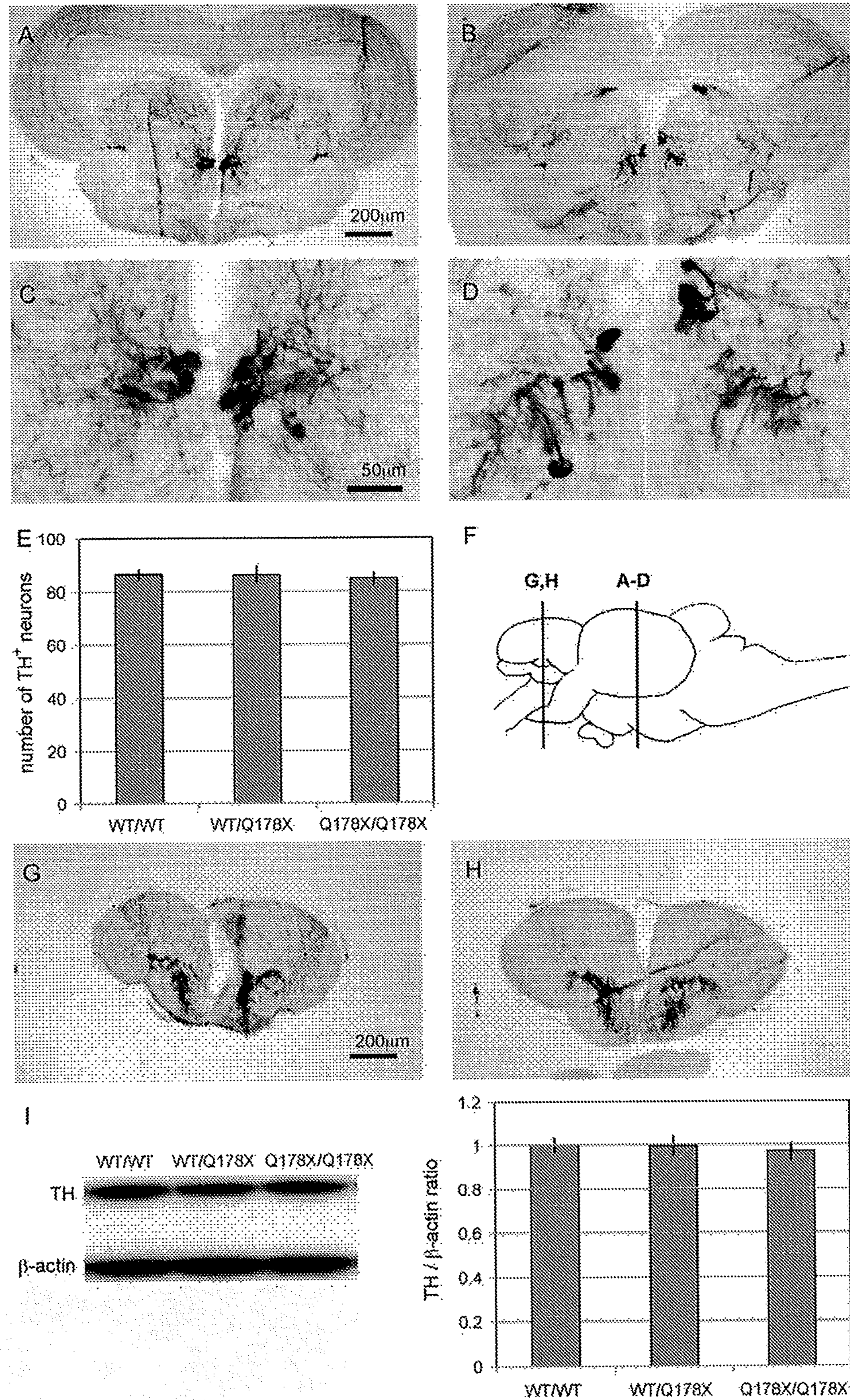

Fig. 8. Immunohistochemistry of tyrosine-hydroxylase and Western blot analysis of *PINK1*$^{Q178X/Q178X}$ medaka. Coronal sections of striatum and middle diencephalon. (A–D) Representative photographs of middle diencephalic dopaminergic neurons in *PINK1*$^{WT/WT}$ (A and C) and *PINK1*$^{Q178X/Q178X}$ (B and D) medaka at 18 months. (E) The number of tyrosine-hydroxylase positive (TH$^+$) neurons does not differ across genotypes (n = 10 for each group). (G) Striatum dopaminergic fibers for *PINK1*$^{WT/WT}$ and (H) *PINK1*$^{Q178X/Q178X}$ medaka at 18 months. The striatum of the *PINK1*$^{Q178X/Q178X}$ medaka is indistinguishable from that of *PINK1*$^{WT/WT}$. (F) Map of medaka brain; A–F indicate the section levels of A–D, F and G. (I) Amount of TH protein in the whole brain at 18 months, examined by Western blot analysis and normalized by β-actin (loading control). The graph shows the ratio of tyrosine-hydroxylase (TH)/β-actin for each genotype (average amount for *PINK1*$^{WT/WT}$ medaka = 1). The amount of TH does not differ across genotypes (n = 6 for each group).

Please cite this article in press as: Matsui, H., et al., Loss of PINK1 in medaka fish (*Oryzias latipes*) causes late-onset decrease in spontaneous movement. Neurosci. Res. (2009), doi:10.1016/j.neures.2009.10.010

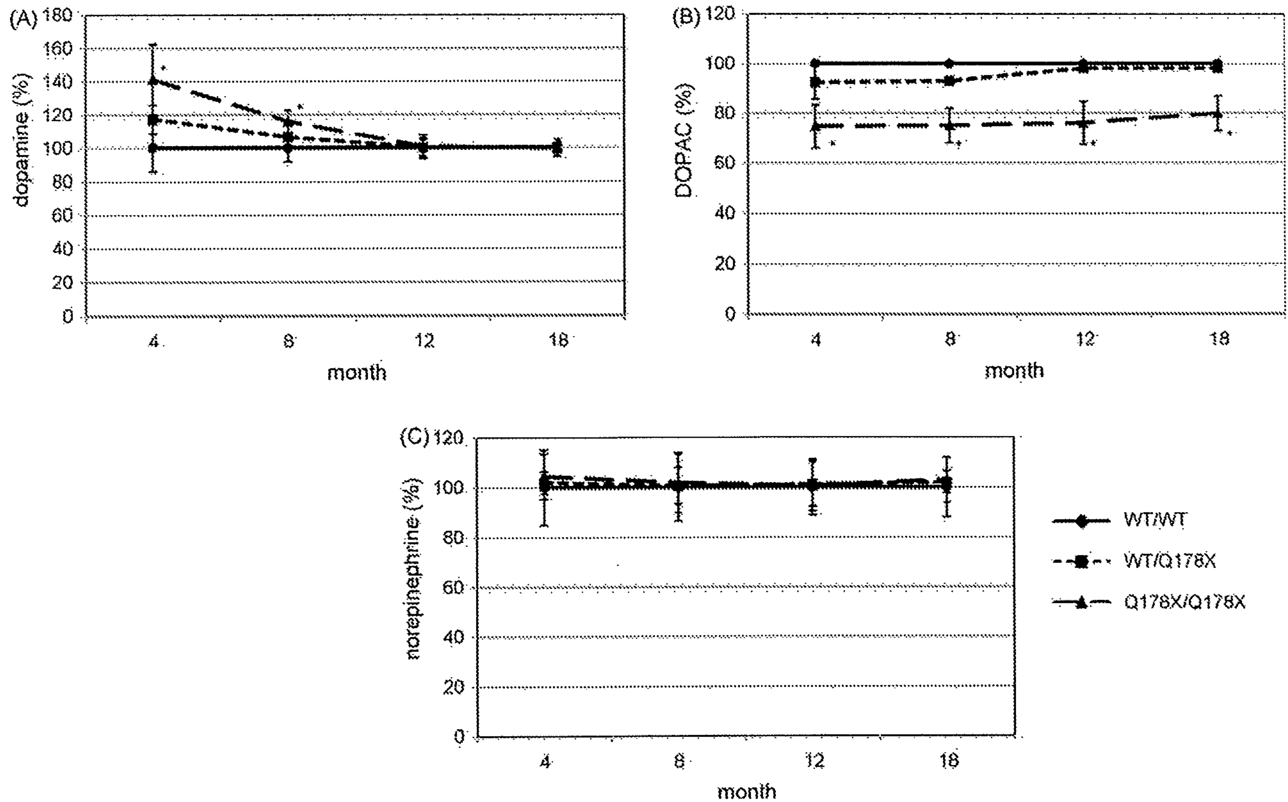

Fig. 9. Amount of dopamine, DOPAC, and norepinephrine in the brain of $PINK1^{Q178X/Q178X}$ medaka. All values are expressed as a percentage of the amount (ng) per protein weight (mg) for $PINK1^{WT/WT}$ ($n = 10$ for each group). (A) The amount of dopamine in the $PINK1^{Q178X/Q178X}$ medaka brain was higher at 4 and 8 months, then registered as normal at 12 and 18 months. (B) The amount of DOPAC decreased at every stage examined. (C) The amount of norepinephrine in the $PINK1^{Q178X/Q178X}$ medaka brain was comparable to that in $PINK1^{WT/WT}$. $^{*}p < 0.05$ vs. $PINK1^{WT/WT}$.

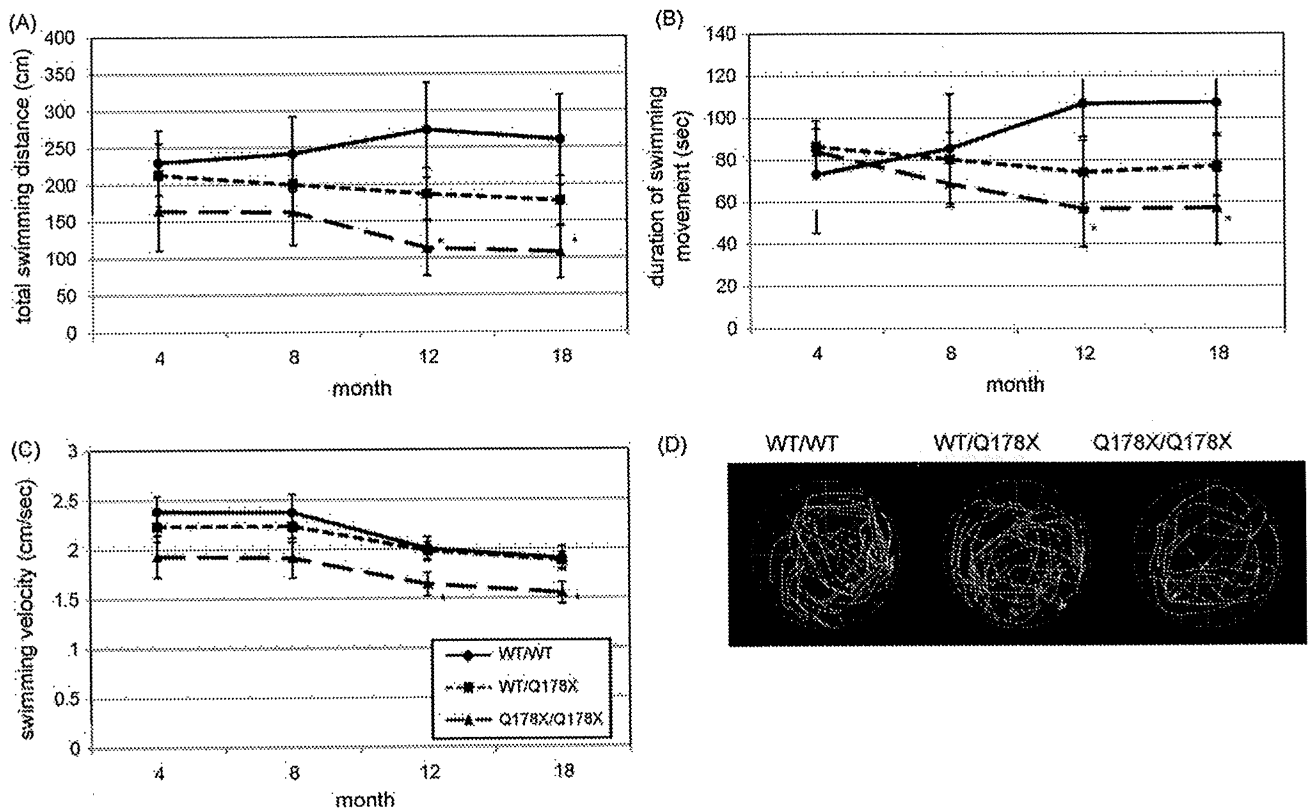

Fig. 10. Spontaneous swimming movement for $PINK1^{Q178X/Q178X}$ medaka. (A) Total swimming distance (cm). (B) Duration of swimming movement (s). (C) Swimming velocity (cm/s). (D) Representative tracks for each genotype. Each genotype showed comparable movement at 4 and 8 months. All parameters for the $PINK1^{Q178X/Q178X}$ medaka decreased at 12 and 18 months ($n = 15$ for each group). $^{*}p < 0.05$ vs. $PINK1^{WT/WT}$.

Please cite this article in press as: Matsui, H., et al., Loss of PINK1 in medaka fish (*Oryzias latipes*) causes late-onset decrease in spontaneous movement. Neurosci. Res. (2009), doi:10.1016/j.neures.2009.10.010

genotype–phenotype relationship include complementing the putative causal allele *in vivo* or *in vitro* by transgenesis or retroviral transduction, non-complementation of a null allele generated by homologous recombination, or backcrossing for many generations to the outcross strain (Cook et al., 2006). Therefore, we conducted the overall experiments using not only 4–6 times back-crossed fish but also fish back-crossed more than 7 times. They all showed the same results, suggesting that loss of PINK1 function indeed resulted in the phenotypes shown in this manuscript. However, we analyzed only a single line of *PINK1* mutant and did not perform rescue experiments using transgenic medaka fish in this study. Therefore further experiments are necessary to elucidate the genotype–phenotype relationship.

In conclusion, this report reveals a new *in vivo* function for PINK1. PINK1 affects the metabolism of dopamine in the brain long before the loss of dopaminergic neurons. PINK1-deficient medaka exhibited decreased spontaneous movement only at the late-adult stage, a phenotype that recapitulates a typical symptom of PD. We recently generated another PD model by treating fish with a chemical neurotoxin, MPTP, a standard method used to induce PD (Matsui et al., 2009). The treatment indeed induced the loss of dopaminergic cells and movement disorder. The medaka PD models can therefore contribute significantly to our understanding of the molecular mechanisms underlying the pathology of PD.

Acknowledgements

We are grateful to the members of the Department of Neurology, Kyoto University, and to Dr. Hideaki Takeuchi and Yuji Suehiro of Tokyo University, for their helpful advice. We thank Prof. Takahiko Yokoyama of the Department of Anatomy and Developmental Biology, Kyoto Prefectural University of Medicine for *in situ* hybridization experiment. We also thank the technical staff of the Department of Radiation Genetics, Kyoto University and the Sequence Technology Team at RIKEN GSC for their assistance.

References

Anichtchik, O., Diekmann, H., Fleming, A., Roach, A., Goldsmith, P., Rubinsztein, D.C., 2008. Loss of PINK1 function affects development and results in neurodegeneration in zebrafish. J. Neurosci. 28, 8199–8207.

Blum, D., Torch, S., Lambeng, N., Nissou, M., Benabid, A.L., Sadoul, R., Verna, J.M., 2001. Molecular pathways involved in the neurotoxicity of 6-OHDA, dopamine and MPTP: contribution to the apoptotic theory in Parkinson's disease. Prog. Neurobiol. 65, 135–172.

Clark, I.E., Dodson, M.W., Jiang, C., Cao, J.H., Huh, J.R., Seol, J.H., Yoo, S.J., Hay, B.A., Guo, M., 2006. *Drosophila* pink1 is required for mitochondrial function and interacts genetically with parkin. Nature 441, 1162–1166.

Cook, M.C., Vinuesa, C.G., Goodnow, C.C., 2006. ENU-mutagenesis: insight into immune function and pathology. Curr. Opin. Immunol. 18, 627–633.

Ekker, S.C., Larson, J.D., 2001. Morphant technology in model developmental systems. Genesis 30, 89–93.

Exner, N., Treske, B., Paquet, D., Holmström, K., Schiesling, C., Gispert, S., Carballo-Carbajal, I., Berg, D., Hoepken, H.H., Gasser, T., Krüger, R., Winklhofer, K.F., Vogel, F., Reichert, A.S., Auburger, G., Kahle, P.J., Schmid, B., Haass, C., 2007. Loss-of-function of human PINK1 results in mitochondrial pathology and can be rescued by parkin. J. Neurosci. 27, 12413–12418.

Gandhi, S., Muqit, M.M., Stanyer, L., Healy, D.G., Abou-Sleiman, P.M., Hargreaves, I., Heales, S., Ganguly, M., Parsons, L., Lees, A.J., Latchman, D.S., Holton, J.L., Wood, N.W., Revesz, T., 2006. PINK1 protein in normal human brain and Parkinson's disease. Brain 129, 1720–1731.

Gasser, T., 2005. Genetics of Parkinson's disease. Curr. Opin. Neurol. 18, 363–369.

Haque, M.E., Thomas, K.J., D'Souza, C., Callaghan, S., Kitada, T., Slack, R.S., Fraser, P., Cookson, M.R., Tandon, A., Park, D.S., 2008. Cytoplasmic Pink1 activity protects neurons from dopaminergic neurotoxin MPTP. Proc. Natl. Acad. Sci. U.S.A. 105, 1716–1721.

Hatano, Y., Li, Y., Sato, K., Asakawa, S., Yamamura, Y., Tomiyama, H., Yoshino, H., Asahina, M., Kobayashi, S., Hassin-Baer, S., Lu, C.S., Ng, A.R., Rosales, R.L., Shimizu, N., Toda, T., Mizuno, Y., Hattori, N., 2004. Novel PINK1 mutations in early-onset parkinsonism. Ann. Neurol. 56, 424–427.

Hedrich, K., Hagenah, J., Djarmati, A., Hiller, A., Lohnau, T., Lasek, K., Grünewald, A., Hilker, R., Steinlechner, S., Boston, H., Kock, N., Schneider-Gold, C., Kress, W., Siebner, H., Binkofski, F., Lencer, R., Münchau, A., Klein, C., 2006. Clinical spectrum of homozygous and heterozygous PINK1 mutations in a large German family with Parkinson disease: role of a single hit? Arch. Neurol. 63, 833–838.

Kitada, T., Asakawa, S., Hattori, N., Matsumine, H., Yamamura, Y., Minoshima, S., Yokochi, M., Mizuno, Y., Shimizu, N., 1998. Mutations in the parkin gene cause autosomal recessive juvenile parkinsonism. Nature 392, 605–608.

Kitada, T., Pisani, A., Porter, D.R., Yamaguchi, H., Tscherter, A., Martella, G., Bonsi, P., Zhang, C., Pothos, E.N., Shen, J., 2007. Impaired dopamine release and synaptic plasticity in the striatum of PINK1-deficient mice. Proc. Natl. Acad. Sci. U.S.A. 104, 11441–11446.

Matsui, H., Taniguchi, Y., Inoue, H., Uemura, K., Takeda, S., Takahashi, R., 2009. A chemical neurotoxin, MPTP induces Parkinson's disease like phenotype, movement disorders and persistent loss of dopamine neurons in the medaka fish (*Oryzias latipes*). Neurosci. Res. 65, 263–271.

Park, J., Lee, S.B., Lee, S., Kim, Y., Song, S., Kim, S., Bae, E., Kim, J., Shong, M., Kim, J.M., Chung, J., 2006. Mitochondrial dysfunction in Drosophila PINK1 mutants is complemented by parkin. Nature 441, 1157–1161.

Pridgeon, J.W., Olzmann, J.A., Chin, L.S., Li, L., 2007. PINK1 protects against oxidative stress by phosphorylating mitochondrial chaperone TRAP1. PLoS Biol. 19, e172.

Sim, C.H., Lio, D.S., Mok, S.S., Masters, C.L., Hill, A.F., Culvenor, J.G., Cheng, H.C., 2006. C-terminal truncation and Parkinson's disease-associated mutations down-regulate the protein serine/threonine kinase activity of PTEN-induced kinase-1. Hum. Mol. Genet. 15, 3251–3262.

Tan, E.K., Yew, K., Chua, E., Puvan, K., Shen, H., Lee, E., Puong, K.Y., Zhao, Y., Pavanni, R., Wong, M.C., Jamora, D., de Silva, D., Moe, K.T., Woon, F.P., Yuen, Y., Tan, L., 2006. PINK1 mutations in sporadic early-onset Parkinson's disease. Mov. Disord. 21, 789–793.

Taniguchi, Y., Takeda, S., Furutani-Seiki, M., Kamei, Y., Todo, T., Sasado, T., Deguchi, T., Kondoh, H., Mudde, J., Yamazoe, M., Hidaka, M., Mitani, H., Toyoda, A., Sakaki, Y., Plasterk, R.H., Cuppen, E., 2006. Generation of medaka gene knockout models by target-selected mutagenesis. Genome Biol. 7, R116.

Taymans, J.M., Van den Haute, C., Baekelandt, V., 2006. Distribution of PINK1 and LRRK2 in rat and mouse brain. J. Neurochem. 98, 951–961.

Unoki, M., Nakamura, Y., 2001. Growth-suppressive effects of BPOZ and EGR2, two genes involved in the PTEN signaling pathway. Oncogene 20, 4457–4465.

Valente, E.M., Abou-Sleiman, P.M., Caputo, V., Muqit, M.M., Harvey, K., Gispert, S., Ali, Z., Del Turco, D., Bentivoglio, A.R., Healy, D.G., Albanese, A., Nussbaum, R., González-Maldonado, R., Deller, T., Salvi, S., Cortelli, P., Gilks, W.P., Latchman, D.S., Harvey, R.J., Dallapiccola, B., Auburger, G., Wood, N.W., 2004. Hereditary early-onset Parkinson's disease caused by mutations in PINK1. Science 304, 1158–1160.

Wood-Kaczmar, A., Gandhi, S., Yao, Z., Abramov, A.S., Miljan, E.A., Keen, G., Stanyer, L., Hargreaves, I., Klupsch, K., Deas, E., Downward, J., Mansfield, L., Jat, P., Taylor, J., Heales, S., Duchen, M.R., Latchman, D., Tabrizi, S.J., Wood, N.W., 2008. PINK1 is necessary for long term survival and mitochondrial function in human dopaminergic neurons. PLoS ONE 3, e2455.

Yang, Y., Gehrke, S., Imai, Y., Huang, Z., Ouyang, Y., Wang, J.W., Yang, L., Beal, M.F., Vogel, H., Lu, B., 2006. Mitochondrial pathology and muscle and dopaminergic neuron degeneration caused by inactivation of *Drosophila* Pink1 is rescued by parkin. Proc. Natl. Acad. Sci. U.S.A. 103, 10793–10798.

Zhou, H., Falkenburger, B.H., Schulz, J.B., Tieu, K., Xu, Z., Xia, X.G., 2007. Silencing of the Pink1 gene expression by conditional RNAi does not induce dopaminergic neuron death in mice. Int. J. Biol. Sci. 3, 242–250.

Please cite this article in press as: Matsui, H., et al., Loss of PINK1 in medaka fish (*Oryzias latipes*) causes late-onset decrease in spontaneous movement. Neurosci. Res. (2009), doi:10.1016/j.neures.2009.10.010

Biochemical and Biophysical Research Communications 391 (2010) 1240–1245

Contents lists available at ScienceDirect

Biochemical and Biophysical Research Communications

journal homepage: www.elsevier.com/locate/ybbrc

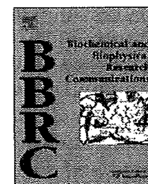

PI3K inhibition causes the accumulation of ubiquitinated presenilin 1 without affecting the proteasome activity

Nobuhisa Aoyagi [a], Kengo Uemura [a,*], Akira Kuzuya [a], Takeshi Kihara [b], Jun Kawamata [a], Shun Shimohama [c], Ayae Kinoshita [d], Ryosuke Takahashi [a]

[a] Department of Neurology, Kyoto University Graduate School of Medicine, Kyoto, Japan
[b] Department of Neuroscience for Drug Discovery, Graduate School of Pharmaceutical Sciences, Kyoto University, Kyoto, Japan
[c] Department of Neurology, School of Medicine, Sapporo Medical University, Kyoto, Japan
[d] School of Health Sciences, Faculty of Medicine, Kyoto University, Kyoto, Japan

A R T I C L E I N F O

Article history:
Received 8 December 2009
Available online 16 December 2009

Keywords:
Alzheimer's disease
γ-Secretase complex
Presenilin 1
Phosphatidylinositol-3 kinase
Proteasome
Ubiquitin

A B S T R A C T

γ-Secretase is an enzymatic complex, composed of presenilin 1 (PS1), nicastrin, pen-2, and aph-1, and is responsible for the intramembranous cleavage of various type-I membrane proteins. The level of each component is tightly regulated in a cell via proteasomal degradation. On the other hand, it has previously been reported that PS1/γ-secretase is involved in the activation of phosphatidylinositol-3 kinase/Akt (PI3K/Akt) pathway. PI3K is inhibited in Alzheimer's disease (AD) brain, whereas the effects of PI3K inhibition on the metabolism of PS1/γ-secretase have not been elucidated. Here, we demonstrate that the treatment of neurons with PI3K inhibitors leads to increased levels of PS1/γ-secretase components through an inhibitory effect on their degradation. Moreover, PI3K inhibition accelerated ubiquitination of PS1. We further show the evidence that the PS1 ubiquitination after PI3K inhibition is represented by the multiple mono-ubiquitination, instead of poly-ubiquitination. Accordingly, treatment of cells with PI3K inhibitor led to a differential intracellular redistribution of PS1 from the one observed after the proteasomal inhibition. These results suggest that PI3K inhibition may trigger the multiple mono-ubiquitination of PS1, which precludes the degradation of PS1/γ-secretase through the proteasomal pathway. Since PS1/γ-secretase is deeply involved in the production of Aβ protein, a deeper knowledge into its metabolism could contribute to a better elucidation of AD pathogenesis.

© 2009 Elsevier Inc. All rights reserved.

Introduction

A major component of the amyloid plaque core in Alzheimer's disease (AD) is the amyloid β peptide (Aβ). γ-Secretase is a protein complex, composed of presenilin 1 or 2 (PS1 or 2), nicastrin, pen-2, and aph-1 and is responsible for the production of Aβ [5,7,9,21]. Recent reports demonstrated that the levels of these four components are tightly regulated each other and, thus, down-regulation of one of these components leads to a decreased level of the whole complex [20]. All of these γ-secretase components can be degraded through the ubiquitin–proteasome system [3,10,11,13,18]. Upon conjugation of polyubiqutin chains to target proteins, proteasome can degrade various proteins including misfolded or aggregated proteins [8,12,24]. On the other hand, multiple mono-ubiquitination of proteins has been attributed to other cellular functions, such as protein trafficking and endocytosis [1,19].

PS1 is a causative gene for familial AD and is considered to be the catalytic core of γ-secretase [6,17,26]. In addition to the well-established role in γ-secretase activity, many reports have shown that PS1 is involved in the activation of phosphatidylinositol-3 kinase/Akt (PI3K/Akt) pathway [2,25], thereby suppressing the activity of glycogen synthase kinase-3β (GSK-3β). Conversely, abnormal activities of GSK-3β have been reported in AD brains [4], indicating that PI3K/Akt pathway is inhibited in AD. Although PS1 has recently been demonstrated to be one of GSK-3β substrates [14,22,23], the effect of PI3K/Akt inhibition on the metabolism of PS1/γ-secretase components has not been demonstrated, yet. To elucidate how PI3K/Akt affects the metabolism of PS1/γ-secretase, we treated mouse primary neurons with PI3K/Akt inhibitors and analyzed their effects on the metabolism of PS1/γ-secretase.

Materials and methods

Cell culture and drug treatment. Primary neurons were obtained from the cerebral cortex of fetal ICR mice (14 days gestation) and cultured in Neurobasal medium supplemented with B27

* Corresponding author. Address: Department of Neurology, Kyoto University School of Medicine, 54 Kawahara-Cho, Shogo-In, Sakyo-Ku, Kyoto 606-8397, Japan. Fax: +81 75 751 9541.
E-mail address: ueken@kuhp.kyoto-u.ac.jp (K. Uemura).

0006-291X/$ - see front matter © 2009 Elsevier Inc. All rights reserved.
doi:10.1016/j.bbrc.2009.12.051

(Invitrogen). Neurons in culture day from 10 to 12 were used for the experiment. HEK293 cells were maintained in Dulbecco's modified Eagle's medium containing 10% fetal bovine serum. For PI3K inhibition, cells were treated with either LY294002 or Wortmannin diluted in the media to give a final concentration of 5 μM and 50 nM, respectively, for an indicated period of time. For the inhibition of Akt, cells were treated with 1 μM Akt inhibitor IV. For proteasome inhibition, cells were treated with 1 μM lactacystin. For inhibition of protein synthesis, cells were treated with 5 μg/mL cycloheximide. Control cells were treated with Dimethylsulfoxide (DMSO).

Construction of plasmids expressing presenilin 1 and ubiquitin mutants and transient transfection. Creation of wild-type human PS1 plasmid was described elsewhere [23]. Human wild-type ubiquitin cDNA with a hemagglutinin (HA) tag (HA-WT-Ub) and HA-tagged ubiquitin whose all lysine residues were replaced with arginine (HA-K0-Ub) were generous gifts from Dr. Y. Imai (Tohoku University). Precise cloning of all reading frames was verified by direct sequencing. Lipofectamine LTX agent (Invitrogen) was used for transient transfection in HEK293 cells according to the manual.

Antibodies and chemical reagents. Rabbit polyclonal anti-PS1 N-terminal fragment (NTF) antibody was from Santa Cruz. Rabbit polyclonal anti-Ubiquitin antibody was from DAKO. Mouse monoclonal anti-PS1 C-terminal fragment (CTF) was from Chemicon. Rabbit polyclonal Anti-nicastrin, mouse monoclonal anti-β-actin, mouse monoclonal anti-β-tubulin, mouse monoclonal anti-γ-tubulin antibodies were from Sigma. Rabbit polyclonal Anti-aph-1 antibody was from Affinity BioReagents. Rat monoclonal Anti-HA tag antibody was from Roche. Donkey polyclonal Anti-mouse and rabbit horseradish peroxidase-conjugated secondary antibodies were from Amersham Biosciences. For immunostaining, Alexa Fluor 546 goat anti-mouse IgG (H + L) conjugate and Alexa Fluor 488 goat anti-rabbit IgG (H + L) conjugate from Molecular Probes were used as secondary antibodies. LY294002 and Wortmannin were from Sigma. AKT inhibitor IV was from Merck. DMSO was from Nacalai Tesque. Lactacystin was from Kyowa Medex. Cycloheximide was from Calbiochem.

Western blotting and immunoprecipitation. The protein levels of γ-secretase components were analyzed by Western blotting as described previously [23]. For immunoprecipitation, cells were washed and scraped like above. NP40 soluble fractions were made by solubilizing the samples in TNE Buffer containing 10 mM Tris-HCl (pH 7.8), 150 mM NaCl, 1% NP40, 1 mM EDTA with proteinase inhibitor cocktail (Roche). Remnant pellets were then further solubilized in TNE buffer plus 1% SDS. After 10-fold dilution of SDS in SDS-free TNE buffer, the samples were subjected to immunoprecipitation. Alternatively, TNE Buffer plus 1% SDS was directly used for cell lysis. Cell lysates containing 1% SDS were diluted 10-fold in SDS-free TNE buffer before immunoprecipitation to avoid degeneration of immunoglobulins. The samples were pretreated with Protein G-Sepharose (GE Healthcare Lifesciences) for an hour at 4 °C to reduce nonspecific binding. After centrifugation, supernatants were collected and precipitating antibodies were added. The samples were rotated at 4 °C for an hour, followed by the addition of new Protein G-Sepharose and rotation for another hour at 4 °C. Immune complexes were washed five times with TNE Buffer. Sample buffer was added to the immune complexes and incubated at room temperature for 10 min. The immunoprecipitated proteins were subjected to SDS–PAGE.

Semi-quantitative reverse transcriptase- polymerase-chain reaction. Total RNA was extracted from primary cultured neurons using ISOGEN (Nippon Gene) and the concentration of RNA was measured by Bio-rad SmartSpec Plus spectrophotometer. The same amount of total RNA was processed for cDNA synthesis using oligo (dT) primers and reverse transcriptase, using TaKaRa RNA LA PCR Kit (AMV) (TaKaRa, Tokyo, Japan). The resulting cDNA was amplified by polymerase-chain reaction. The primers used were 5′-GGT ACCCAAGAACCCCAAGT-3′ and 5′-CCGGGTCTTCACTCGTTAGA-3′ for mouse presenilin 1, 5′-GGAACCAACTTCAGCAGCTC-3′ and 5′-GAGCCTCTCTGTCCTGTTGG-3′ for mouse nicastrin, 5′-ACCACAGTCC ATGCCATCAC-3′ and 5′-TCCACCACCCTGTTGCTGTA-3′ for mouse GAPDH. The number of cycle was optimized so as to avoid saturation of amplified DNA as previously described [15].

Proteasome activity assay. Proteasome activity was quantified by the measurement of the release of 7-amino-4-methylcoumarin from the fluorogenic peptide Suc-Leu-Leu-Val-Tyr-7-amino-4-methylcoumarin (Suc-LLVY-AMC, Affinity Research Product). Primary cultured neurons were washed twice with phosphate-buffered saline (PBS), harvested on ice, and resuspended into a buffer containing 25 mM Hepes and 0.5 mM EDTA. Cells were centrifuged and lysed by brief sonication. SDS solution was added to the lysate to give the final concentration of 0.03%. Then the fluorogenic substrate Suc-Leu-Leu-Val-Tyr-7-amino-4-methylcoumarin was added to the mixture and incubated at 37 °C for 30 min. Proteasome activity was detected by changes in fluorescence intensity at 355 nm of excitation and 460 nm of emission using an automatic multi-well plate reader. The relative activity was standardized by protein concentration, which was determined using BCA protein assay kit (Pierce).

Immunostaining. Cells were fixed with 4% paraformaldehyde for 20 min. Fixed cells were blocked with 3% BSA in PBS with 0.2% Triton X-100 for 15 min and incubated overnight at 4 °C with each antibody diluted in PBS containing 3% BSA. Immunoreactivity was visualized using the species-specific secondary antibodies mentioned above. Samples were examined using a LSM (Zeiss) confocal scanning microscope.

Statistical analysis. The relative density of the bands in Western blotting was analyzed by quantitative densitometry using a computerized image analysis program (NIH image 1.59). To compare the ratios of each γ-secretase component to β–actin between treatments, Student's *t*-test was used for the analysis. The mRNA levels of γ-secretase components and the proteasomal activity were analyzed by using One-way Factorial ANOVA, followed by post hoc Fisher's protected least significant difference. Quantified data were expressed as the means ± SD, and significance was assessed at $P < 0.05$.

Results and discussion

We first investigated the effect of PI3K/Akt activity on the metabolism of γ-secretase. To test this, primary cultured mouse neurons were treated with either vehicle (DMSO) or a PI3K inhibitor, LY294002 for 48 h. Immunoblotting of the cell lysate demonstrated increased levels of γ-secretase components (PS1, nicastrin, Pen-2, Aph-1) upon PI3K inhibition (Fig. 1A, left). The quantitative analysis of each γ-secretase component band intensity revealed significant increase after the LY294002 treatment (Fig. 1A, right, $n = 3$, $p < 0.05$). Similarly, inhibition of Akt activity by a treatment with Akt inhibitor IV for 24 h caused an accumulation of γ-secretase complex components (Fig. 1B). The statistical analysis of three independent experiments showed a significant increase of every γ-secretase component after Akt inhibition ($p < 0.05$, data not shown), validating the involvement of PI3K/Akt pathway in the regulation of γ-secretase components protein levels.

We then asked whether this accumulation is due to an accelerated transcription of γ-secretase components or, alternatively, an inhibition on the degradation machinery of the components. To answer this question, we analyzed the mRNA levels of γ-secretase components (PS1 and nicastrin) under PI3K inhibition by semi-quantitative RT-PCR. Mouse primary cultured neurons were treated with either vehicle or one of PI3K inhibitors (Wortmannin or LY294002) for 24 h. Total mRNA was extracted from the cell

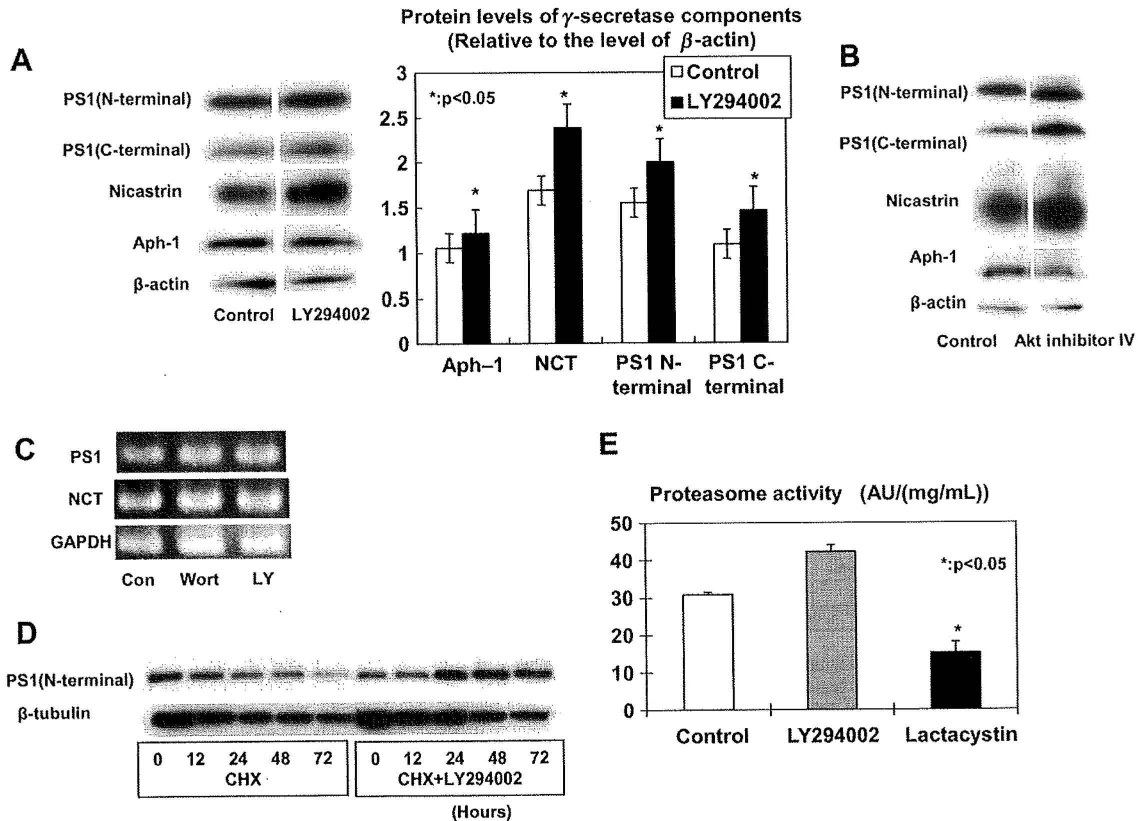

Fig. 1. The level of PS1/γ-secretase complex increases upon an inhibition of PI3K/Akt pathway (A) Mouse cortical neurons in primary culture were treated with either vehicle (DMSO) or LY294002 for 48 h. The cells were collected and cell lysates were subjected to immunoblotting by anti-PS1 (N-terminal, C-terminal), Nicastrin, Aph-1, or β-actin antibodies (left). The band intensity of each γ-secretase component is normalized by that of β-actin and analyzed by Student's *t*-test. The level of each component was significantly higher in the cells treated with LY294002 compared to that in the cells treated with vehicle (right, $n = 3$, $p < 0.05$). (B) Mouse cortical neurons in primary culture were treated with either vehicle (DMSO) or AKT inhibitor IV for 24 h. Cells were collected and immunoblotted with antibodies against anti-PS1 (N-terminal, C-terminal), Nicastrin, Aph-1, or β-actin. (C) Mouse cortical neurons in primary culture were treated with vehicle, Wortmannin or LY294002 for 24 h. Cells were collected and the total RNA was extracted from the cell lysates. mRNA levels were semi-quantified by RT-PCR. The mRNA levels of γ-secretase components was normalized to that of GAPDH and analyzed by One-way Factorial ANOVA ($n = 3$). (D) Mouse cortical neurons in primary culture were treated with CHX alone or CHX together with LY294002. Cells were collected 0. 12, 24, 48, 72 h after the treatment. Cell lysates were subjected to immunoblotting by anti-PS1 antibody. The expression level of PS 1 decreased along with the time after CHX treatment. Co-treatment of cells with CHX and LY294002 inhibited the decrease of PS1. β-tubulin levels were consecutively decreased after CHX treatment regardless of the presence of LY294002. (E) Primary culture neurons were treated with vehicle, LY294002 or lactacystin for 24 h. Proteasomal activity defined by release of 7-amino-4-methylcoumarin from the fluorogenic peptide Suc-Leu-Leu-Val-Tyr-7-amino-4-methylcoumarin was measured by fluorescence intensity. Only lactacystin treatment showed significant decrease in proteasome activity ($n = 3$, One-way Factorial ANOVA).

pellets, followed by the RT-PCR analyses of PS1, nicastrin and β-actin mRNA levels (Fig. 1C). We observed no significant difference between the vehicle and a PI3K inhibitor (Wortmannin or LY294002) treatment groups with respect to the mRNA levels of PS1 and nicastrin ($n = 3$). These results indicate that the transcriptions of PS1 and nicastrin were not affected by PI3K inhibition.

We then examined whether PI3K inhibition cause an altered degradation activity of PS1 in neurons, using a protein synthesis inhibitor, cycloheximide (CHX). Mouse primary cultured neurons were incubated with CHX in the presence or absence of LY294002 for 0, 12, 24, 48, 72 h. The protein levels of PS1 and β-tubulin gradually decreased by the treatment with CHX alone, reflecting the protein degradation in the absence of new protein synthesis (Fig. 1D, top, left). On the contrary, simultaneous treatment of cells with CHX and LY294002 maintained the amount of PS1 up to 72 h after the treatment (Fig. 1D, top, right). These results indicate that PI3K inhibition precludes the degradation of PS1 to stabilize its protein expression. Conversely, the decrease in cellular β-tubulin levels was comparable between the cells treated with CHX alone and the cells simultaneously treated with CHX and LY294002 (Fig. 1D, bottom), indicating LY294002 specifically stabilize the level of PS1.

In order to rule out a possibility that PI3K inhibition caused general inhibition of proteasome activity, thereby non-specifically inhibiting the degradation of γ-secretase components as well as many other proteins, we measured the proteasome activity within mouse primary cultured neurons under PI3K inhibition. Mouse primary cultured neurons were treated with vehicle, LY294002, or lactacystin, a specific proteasome inhibitor, for 24 h followed by the measurement of proteasome activity (Fig. 1E). There was no significant difference in proteasome activity between in the cells treated with the vehicle and LY294002, whereas significant decrease in proteasome activity was observed in the cells treated with lactacystin. Thus, LY294002 stabilizes PS1/γ-secretase components by specifically inhibiting their degradation.

Since the level of PS1 is regulated by the ubiquitin–proteasome system [13,18], we postulated that PI3K inhibition could have altered the ubiquitination status of PS1, thereby stabilizing its protein level. To test this, HEK293 cells were transfected with wild-type PS1 and treated with either PI3K inhibitors (Wortmannin or LY294002) or proteasome inhibitor (lactacystin). After the treatment, cell lysates were fractionated into NP40 soluble or insoluble fractions. Each fraction was immunoprecipitated with anti-PS1 antibody, followed by Western blotting with anti-ubiquitin